

Learning Lévy density via adaptive RKHS regression with bi-level optimization

Luxuan Yang[†], Fei Lu^{*}, Ting Gao[‡], Wei Wei[§] and Jinqiao Duan[¶]

Abstract

We propose a nonparametric method to learn the Lévy density from probability density data governed by a nonlocal Fokker–Planck equation. We recast the problem as identifying the kernel in a nonlocal integral operator from discrete data, which leads to an ill-posed inverse problem. To regularize it, we construct an adaptive reproducing kernel Hilbert space (RKHS) whose kernel is built directly from the data. Under standard source and spectral decay conditions, we show that the reconstruction error decays in the mesh size at a near optimal rate. Importantly, we develop a generalized singular value decomposition (GSVD)-based bilevel optimization algorithm to choose the regularization parameter, leading to efficient and robust computation of the regularized estimator. Numerical experiments for several Lévy densities, drift fields and data types (PDE-based densities and sample ensemble-based KDE reconstructions) demonstrate that our bilevel RKHS method outperforms classical L-curve and generalized cross-validation strategies and that the adaptive RKHS norm is more accurate and robust than L^2_ρ - and ℓ^2 -based regularization.

Keywords: Inverse problem; Lévy measure; bi-level optimization; RKHS; nonlocal operator

Contents

1 Introduction	2
2 Adaptive kernel regression and regularization	4
3 Convergence of the RKHS-regularized estimator	9
4 Hyperparameter selection via Bi-level optimization	13

[†]School of Mathematics and Statistics & Center for Mathematical Sciences, Huazhong University of Science and Technology, Wuhan 430074, China. Email: luxuan_yang@hust.edu.cn

^{*}Department of Mathematics, Johns Hopkins University, Baltimore, USA. Email: feilu@math.jhu.edu

[‡]School of Mathematics and Statistics & Center for Mathematical Sciences, Huazhong University of Science and Technology, Wuhan 430074, China. Email: tgao0716@hust.edu.cn

[§]College of Mathematics and Statistics, Chongqing University, Chongqing 401331, China. Email: weiw@cqu.edu.cn

[¶]Department of Mathematics and Department of Physics, Great Bay University, Dongguan, Guangdong 52300, China. Email: duan@gbu.edu.cn

^{*}is the corresponding author

5	Numerical experiments	16
6	Conclusion	23
A	Appendix: technical results and proofs	24

1 Introduction

We consider the problem of estimating the Lévy density ϕ of a Lévy motion L_t appearing in the one-dimensional SDE

$$dX_t = b(X_t) dt + \sigma(X_t) dB_t + dL_t \tag{1.1}$$

from data consisting of the probability density $p(x, t)$ of X_t on a discrete space-time mesh or from reconstructed densities based on observed sequences of sample ensembles. Here, the drift $b : \mathbb{R}^1 \rightarrow \mathbb{R}^1$ and the diffusion $\sigma : \mathbb{R}^1 \rightarrow \mathbb{R}^1$ are known functions, L_t is a scalar and symmetric Lévy motion with generating triplet $(0, 0, \nu)$ independent of a scalar Brownian motion B_t and its Lévy jump measure ν admits a symmetric density ϕ with respect to Lebesgue measure, i.e. $d\nu(x) = \phi(x) dx$.

Identifying ϕ is practically important because it specifies the Lévy jump measure ν and thereby characterizes the jump properties of the Lévy process L_t , with applications to modeling volatility jumps in financial markets [1–3] and analyzing changes in climate systems [4, 5].

A broad literature estimates Lévy measures from trajectory data of the Lévy process rather than from densities. In high-frequency (in time) settings, Comte and Genon-Catalot [6] estimate $g(y) = y\phi(y)$ via frequency-domain and projection methods based on the characteristic function of increments, under asymptotics $\Delta t \rightarrow 0$ and $N\Delta t \rightarrow \infty$. However, recovering $\phi(y) = g(y)/y$ then becomes unstable near $y = 0$. In low-frequency regimes, Neumann and Reiß [7] estimate Lévy–Khinchine characteristics from characteristic functions and their derivatives, but show that the diffusion coefficient cannot be uniformly consistently recovered without extra assumptions, which obstructs a unique reconstruction of ϕ . Pathwise approaches based on the Lévy–Itô decomposition, such as [8], extract jump information from thresholded high-frequency increments and then estimate a compound Poisson approximation; these methods require carefully tuned thresholds and high sampling rates to control contamination by small jumps. More recently, several works focus on estimating increment densities rather than ϕ itself, e.g., [9, 10].

To address cases of density data without trajectory information, an alternative approach uses the Fokker–Planck equation and nonlocal Kramers–Moyal formulas. Li and Duan [11] fit parametric Lévy families using small-time transition probabilities and conditional moments without explicitly solving (1.2), while Lu et al. [12] approximate transition densities via normalizing flows and then infer a stability index within a prespecified Lévy family. These approaches exploit the nonlocal generator but remain confined to parametric estimation. Parallel to this, there is a growing literature on learning nonlocal operators from data: many works treat the operator as a black box to be approximated by neural networks [13, 14], while others learn parametric kernels in nonlocal models (e.g., Bernstein polynomials with ℓ^2 regularization [15, 16]). To improve flexibility, Lu et al. [17] proposed a data-adaptive RKHS Tikhonov regularization framework for learning the kernel. However, the impact of mesh-dependent discretization errors and the principled selection of regularization parameters remain to be further explored.

In this work, we learn ϕ by exploiting the Fokker–Planck equation for $p(x, t)$:

$$\partial_t p = -\partial_x(bp) + \frac{1}{2}\partial_{xx}(\sigma^2 p) + \int_{\mathbb{R}^1 \setminus \{0\}} [p(x+y, t) - p(x, t)] \phi(|y|) dy, \tag{1.2}$$

and regard ϕ as an unknown kernel in a nonlocal operator to be inferred from data $\mathcal{D} = \{p_{t_i}(x_j)\}_{i,j=1}^{N,J}$ on a uniform spatial grid $\{x_j\} \subset \Omega_{R_0}$ and observation times $\{t_i\}$. To make the nonlocal integral numerically tractable, we assume that ϕ is supported on $(0, R_0]$ (a standard modeling choice; see, e.g., [6, 18]) and restrict x to $\Omega_{R_0} := \{z \in \Omega : [z - R_0, z + R_0] \subset \Omega\}$ so that $x \pm y \in \Omega$ for all $|y| \leq R_0$. In this setting, recovering ϕ from discrete data and the numerical errors in estimating the derivatives of p leads to an ill-posed inverse problem. This makes regularization indispensable and motivates a mesh-dependent error analysis.

Based on the above formulation, we develop a nonparametric regression framework to learn ϕ from data using the data-adaptive RKHS Tikhonov regularization of [17] with a principled bi-level optimization scheme for selecting the regularization hyperparameter. Specifically, from data, we construct an adaptive reproducing kernel \overline{G} whose associated integral operator is precisely the Hessian of the quadratic loss for ϕ . This leads to an RKHS $H_{\overline{G}}$ that (i) is tailored to the analytic structure of the nonlocal operator, (ii) automatically restricts estimation to the subspace of identifiability, and (iii) provides a natural regularization norm.

Notably, we derive a mesh-dependent error bound for the RKHS-regularized estimator and show that, with an optimally chosen regularization parameter, the reconstruction error decays like $(\Delta x)^{\frac{2\beta\varsigma}{2\beta\varsigma+4\varsigma+1}}$ before saturation, where β is the smooth exponent in a source condition and ς is the power exponent of spectral decay. This extends the optimal order of Tikhonov regularization (e.g., [19, Sec. 3.2]) to a setting where the normal operator and the data are both discretized and the regularization uses an adaptive RKHS norm. When numerical quadrature errors are negligible, our rates become comparable (up to minor exponent differences due to the different effective dimension scalings) to the minimax optimal rates for inverse statistical learning in [20] and the statistical inverse problem with DA-RKHS regularization in [21], while explicitly quantifying how spatial discretization degrades the reconstruction accuracy.

Importantly, we develop a generalized singular value decomposition (GSVD)-based bi-level optimization scheme to select the regularization hyperparameter from data. In our bi-level optimization, the lower level solves a Tikhonov-regularized least-squares problem, for which GSVD yields both the closed-form solution and the inverse-Hessian needed to compute hypergradients in the upper-level update. Thus, while it is inspired by recent bi-level optimization approaches [22, 23], our *bilevel-RKHS* approach avoids repeated computation inverse-Hessian and gives a stable, efficient hyperparameter selection procedure.

Numerically, we show that the *bilevel-RKHS* outperforms classical L-curve [24] and generalized cross-validation [25] strategies and that the adaptive RKHS norm is superior to L_ρ^2 - and ℓ^2 -based regularization across multiple Lévy densities, drift fields, and data types (PDE-based density snapshots and sample ensemble-based KDE reconstructions).

Our contributions can be summarized as follows:

- We formulate the recovery of Lévy density ϕ from the nonlocal Fokker–Planck operator as an ill-posed inverse problem, and construct an automatic adaptive RKHS $H_{\overline{G}}$ that encodes identifiability and provides a principled regularization norm.
- We establish mesh-dependent convergence rates for the RKHS-regularized estimator under suitable source and spectral decay conditions, explicitly capturing the effect of spatial discretization (Δx) on the reconstruction error.
- We design an efficient GSVD-based bi-level RKHS algorithm for selecting the regularization hyperparameter with closed-form hypergradients, and demonstrate its numerical

advantages over L-curve and GCV, as well as over alternative norms.

Beyond the specific task of Lévy density estimation, our framework contributes to the broader program of learning nonlocal operators and ill-posed inverse problems from data. It combines structure-exploiting operator learning, adaptive function spaces, and bilevel hyperparameter optimization and can be extended in several directions: to higher-dimensional Lévy processes and to joint nonparametric recovery of drift, diffusion, and jump components. We view this work as a step toward data-adaptive learning of stochastic dynamics with jumps, and anticipate that the GSVD-based bilevel selection of hyperparameters will be useful in a range of nonlocal operator learning problems.

Our paper is organized as follows. In Section 2, we formulate the inverse problem, define the adaptive RKHS and its discrete approximation. Section 3 establishes convergence rates for the RKHS-regularized estimator. We present in Section 4 the bi-level optimization algorithm, and report numerical experiments for different Lévy densities and data-generation scenarios in Section 5. Section 6 concludes and discusses possible extensions.

Preliminaries and notations. Here, we briefly introduce the definitions and notation used throughout the paper.

Lévy Process: Let $X = (X(t), t \geq 0)$ be a stochastic process defined on a probability space (Ω, \mathcal{F}, P) . We say that X is a *Lévy process* if: (i) $X(0) = 0$ (a.s); (ii) X has independent and stationary increments; (iii) X is stochastically continuous, i.e. for all $a > 0$ and all $s \geq 0$, $\lim_{t \rightarrow s} P(|X(t) - X(s)| > a) = 0$.

Lévy Measure: Let ν be a Borel measure defined on $\mathbb{R}^d \setminus \{0\}$. We say that it is a *Lévy measure* if $\int_{\mathbb{R}^d \setminus \{0\}} (|y|^2 \wedge 1) \nu(dy) < \infty$. If the Lévy measure ν is absolutely continuous with respect to Lebesgue measure, the Radon-Nikodym derivative $\phi = d\nu/dx$ is called the *Lévy density*. Then, when Lévy Process is symmetric, Lévy Measure ν is symmetric so that Lévy density is .

Symmetric Lévy process: A Lévy process X is called *symmetric* if $L_t = -L_t$ for all $t \geq 0$. In this case, the Lévy measure is symmetric in the sense that $\nu(A) = \nu(-A)$ for all Borel sets $A \subset \mathbb{R} \setminus \{0\}$. Consequently, If the Lévy measure ν is absolutely continuous, the Lévy density satisfies $\phi(y) = \phi(-y)$ for a.e. $y \neq 0$.

The whole paper follows the notation in Table 1.

Table 1: Table of notations

$\bar{\mathbf{A}}$ and $\bar{\mathbf{A}}^M$	normal matrices of continuum and discrete data
$\bar{\mathbf{b}}$ and $\bar{\mathbf{b}}^M$	normal vectors of continuum and discrete data
$\mathbf{G}, \mathbf{Q}, \mathbf{U}, \mathbf{X}, \mathbf{K}, \mathbf{M}$	matrix or array by bold capital letters
\mathbf{f}, \mathbf{c}	vector by bold lowercase letters
γ, λ	scalar by Greek letters

2 Adaptive kernel regression and regularization

Assuming continuum-in-space data, we first formulate the estimation of the Lévy density as a variational inverse problem. We then show that the problem is ill-posed and propose an adaptive RKHS framework for regression and regularization. Throughout, we assume that the Lévy density ϕ is symmetric and has bounded support in $(-R_0, R_0)$, a standard assumption (see, e.g., [18]) and we focus on the computationally practical case $R_0 < \infty$.

2.1 Regression estimator

We recover the Lévy density by solving an inverse problem of learning the convolution kernel in the integral operator of the Fokker-Planck equation. Specifically, with p_t denoting the probability density of X_t , we define $R_\phi[p_t]$ the a nonlocal operator parametrized by the Lévy density ϕ :

$$R_\phi[p_t](x) := \int_{\Omega} \phi(|y|)[p_t(y+x) - p_t(x)]dy = \int_{(0, R_0]} \phi(r)Q[p_t](x, r)dr, \quad (2.1)$$

for $x \in \Omega_{R_0} := \{z \in \Omega : [z - R_0, z + R_0] \in \Omega\}$, and the functional $Q[p_t] : \Omega_{R_0} \times (0, R_0] \rightarrow \mathbb{R}$ is

$$Q[p_t](x, r) = p_t(x+r) + p_t(x-r) - 2p_t(x), r \in (0, R_0], x \in \Omega_{R_0}. \quad (2.2)$$

Note that the evaluation of $R_\phi[p_t](x)$ with $x \in \Omega_{R_0}$ uses the values of p_t in Ω .

The task is to estimate the function ϕ of the nonlocal operator R_ϕ in the following reformulation of the Fokker-Planck equation

$$R_\phi[p_t](x) = f_t(x) := \frac{\partial p_t(x)}{\partial t} + \frac{\partial}{\partial x} [b(x)p_t(x)] - \frac{1}{2} \frac{\partial^2 [\sigma(x)^2 p_t(x)]}{\partial x^2}. \quad (2.3)$$

We assume first that we have continuum data of function pairs:

$$\mathcal{T} = \{(p_{t_i}(x)_{x \in \Omega}, f_{t_i}(x)_{x \in \Omega_{R_0}})\}_{i=1}^N. \quad (2.4)$$

Consider the minimizer of the loss function of mean square error:

$$\hat{\phi}_{H_n} = \arg \min_{\phi \in H_n} \mathcal{E}_\infty(\phi), \quad \text{where} \quad \mathcal{E}_\infty(\phi) = \frac{1}{N} \sum_{i=1}^N \int_{\Omega_{R_0}} |R_\phi[p_{t_i}](x) - f_{t_i}(x)|^2 dx. \quad (2.5)$$

Here, the hypothesis space $H_n = \text{span} \{\phi_k\}_{k=1}^n$ with basis functions $\{\phi_k\}$ will be selected in the next sections using an adaptive RKHS. For each $\phi = \sum_{k=1}^n c_k \phi_k \in H_n$, noticing that $R_\phi = \sum_{k=1}^n c_k R_{\phi_k}$, we can write the loss function as :

$$\begin{aligned} \mathcal{E}_\infty(\phi) &= \frac{1}{N} \sum_{i=1}^N \int_{\Omega_{R_0}} \left| \sum_{k=1}^n c_k R_{\phi_k}[p_{t_i}](x) - f_{t_i}(x) \right|^2 dx \\ &= \mathbf{c}^\top \bar{\mathbf{A}} \mathbf{c} - 2\mathbf{c}^\top \bar{\mathbf{b}} + C_N^f =: \mathcal{E}(\mathbf{c}), \end{aligned} \quad (2.6)$$

where $\mathbf{c} = (c_1, \dots, c_n)^\top$, the normal matrix and vectors are

$$\begin{aligned} \bar{\mathbf{A}}(k, k') &= \frac{1}{N} \sum_{i=1}^N \int_{\Omega_{R_0}} R_{\phi_k}[p_{t_i}](x) R_{\phi_{k'}}[p_{t_i}](x) dx, \quad 1 \leq k, k' \leq n \\ \bar{\mathbf{b}}(k) &= \frac{1}{N} \sum_{i=1}^N \int_{\Omega_{R_0}} R_{\phi_k}[p_{t_i}](x) f_{t_i}(x) dx, \quad 1 \leq k \leq n, \end{aligned} \quad (2.7)$$

and $C_N^f = \frac{1}{N} \sum_{i=1}^N \int_{\Omega_{R_0}} |f_{t_i}(x)|^2 dx$ is a constant. Hence, a minimizer for (2.5), which is a least squares estimator(LSE) with a minimal coefficient norm, is $\hat{\phi}_{H_n} = \sum_{k=1}^n \hat{c}_k \phi_k$ with $\hat{\mathbf{c}} = \bar{\mathbf{A}}^\dagger \bar{\mathbf{b}}$, where $\bar{\mathbf{A}}^\dagger$ is pseudo-inverse of $\bar{\mathbf{A}}$.

Regularization is necessary in practice since the normal matrix $\bar{\mathbf{A}}$ is often ill-conditioned and the normal vector $\bar{\mathbf{b}}$ is perturbed by sampling error or numerical integration error. In fact, as we will show in the next section, the underlying inverse problem is ill-posed.

Before picking a proper regularization norm, we must first address a fundamental issue: defining the function space for estimating ϕ . Subsequently, we define function spaces adaptive to this inverse problem, characterize its ill-posedness, and propose an adaptive RKHS for regularization.

2.2 An adaptive RKHS for regression and regularization

Since we have little prior information about the Lévy density, we define function spaces adaptive to this variational approach through the lens of statistical learning, as in [17, 26, 27]. In particular, we characterize the ill-posedness of this variational inverse problem using the loss function's Hessian and define an adaptive RKHS for regression. Moreover, we assume uniform boundedness of continuum data, which often holds, for example, when the diffusion term is uniformly elliptic so the density is smooth [28].

Assumption H1 *The continuum data $\{p_{t_i}\}_{i=1}^N$ satisfy that*

$$C_{max} := \max_i \sup_{x \in \Omega} p_{t_i}(x) < \infty, \quad Z := \int_0^{R_0} \frac{1}{N} \sum_{i=1}^N \int_{\Omega_{R_0}} |Q[p_{t_i}](x, r)| dx dr < \infty, \quad (2.8)$$

where $Q[p_t]$ is defined in (2.2).

Given data $\{p_{t_i}(x)\}_{i=1}^N$ satisfying Assumption H1, let ρ be the measure on $(0, R_0]$ whose density function with respect to the Lebesgue measure is

$$\rho(r) = \frac{1}{ZN} \sum_{i=1}^N \int_{\Omega_{R_0}} |Q[p_{t_i}](x, r)| dx. \quad (2.9)$$

The measure ρ quantifies the strength that the data explores ϕ . In particular, outside of its support, the data provides no information about ϕ . Thus, we call it an *exploration measure*, and set the default function space of estimating ϕ to be L_ρ^2 .

We define a function $\bar{G} : [0, R_0] \times [0, R_0] \rightarrow \mathbb{R}$ as

$$\bar{G}(r, s) = \frac{G(r, s)}{\rho(r)\rho(s)} \mathbf{1}_{\{\rho(r)\rho(s) > 0\}}, \quad G(r, s) = \frac{1}{N} \sum_{i=1}^N \int Q[p_{t_i}](x, r) Q[p_{t_i}](x, s) dx, \quad (2.10)$$

where ρ is the exploration measure defined in (2.9).

The next lemma shows that \bar{G} is a positive semi-definite and square-integrable function, so its integral operator $\mathcal{L}_{\bar{G}}$ is compact. In particular, the variational inverse problem of minimizing the quadratic loss function in (2.5) is ill-posed since it involves the inversion of the operator $\mathcal{L}_{\bar{G}}$. We postpone its proof to Appendix A.

Lemma 2.1 *Given data $\{p_{t_i}\}_{i=1}^N$ satisfying Assumption H1, the function \bar{G} in (2.10) is a positive semi-definite function and $\bar{G} \in L^2(\rho \otimes \rho)$. Consequently, its integral operator $\mathcal{L}_{\bar{G}} : L_\rho^2 \rightarrow L_\rho^2$*

$$\mathcal{L}_{\bar{G}}\phi(r) = \int_0^{R_0} \phi(s) \bar{G}(r, s) \rho(s) ds, \quad \forall \phi \in L_\rho^2 \quad (2.11)$$

is compact, positive semi-definite. Furthermore, the loss function in (2.5) can be written as

$$\mathcal{E}_\infty(\phi) = \langle \mathcal{L}_{\bar{G}}\phi, \phi \rangle_{L_\rho^2} - 2\langle \phi^D, \phi \rangle_{L_\rho^2} + C, \quad (2.12)$$

and its minimizer in $\text{Null}(\mathcal{L}_{\bar{G}})^\perp$ is $\hat{\phi} = \mathcal{L}_{\bar{G}}^{-1}\phi^D$. Here, the function $\phi^D \in L_\rho^2$ is the Riesz representation of the bounded linear functional

$$\langle \phi^D, \phi \rangle_{L_\rho^2} = \frac{1}{N} \sum_{i=1}^N \int R_\phi[p_{t_i}](x) f_{t_i}(x) dx, \quad \forall \phi \in L_\rho^2. \quad (2.13)$$

Therefore, the inverse problem of minimizing the loss function is ill-posed, and it is crucial to regularize the problem by seeking solutions in $\text{Null}(\mathcal{L}_{\bar{G}})^\perp$. We introduce the following RKHS for regularization.

Definition 2.2 (Adaptive RKHS) *We call \bar{G} in (2.10) the automatic reproducing kernel for the inverse problem of learning the density of the Lévy measure ϕ in the operator R_ϕ in (2.1) from data $\{p_{t_i}\}_{i=1}^N$ satisfying Assumption H1. Its associated RKHS, denoted by $H_{\bar{G}}$, is called an adaptive RKHS.*

The RKHS $H_{\bar{G}}$ is data-adaptive since its reproducing kernel \bar{G} adjusts to the continuum data. It is well-known that the RKHS can be expressed as $H_{\bar{G}} := \mathcal{L}_{\bar{G}}^{-1/2}(L_\rho^2)$; see e.g., [17, 21, 29].

Notably, the closure of $H_{\bar{G}}$ coincides with $\text{Null}(\mathcal{L}_{\bar{G}})^\perp$, within which the loss function admits a unique minimizer, making it an ideal space for regularization. Consequently, the RKHS $H_{\bar{G}}$ naturally leads to the derivation of a regularized estimator:

$$\hat{\phi}_\lambda = \arg \min_{\phi \in H_{\bar{G}}} \mathcal{E}_\lambda(\phi), \quad \mathcal{E}_\lambda(\phi) := \mathcal{E}_\infty(\phi) + \lambda \|\phi\|_{H_{\bar{G}}}^2. \quad (2.14)$$

Here, λ is a hyperparameter controlling the strength of regularization.

In particular, we can also use \bar{G} kernel regression. That is, setting the basis function of the hypothesis $H_n = \text{span}\{\phi_k\}_{k=1}^n$ to be

$$\phi_k(r) = \bar{G}(r_k, r), \quad 1 \leq k \leq n, \quad (2.15)$$

where $\{r_k\}_{k=1}^n \subset (0, R_0]$ are mesh points, we have, by the reproducing property, for any $\phi(r) = \sum_{k=1}^n c_k \bar{G}(r_k, r) \in H_n$,

$$\|\phi\|_{H_{\bar{G}}}^2 = \sum_{k=1}^n \sum_{m=1}^n c_k c_m \langle \bar{G}(r_k, r), \bar{G}(r_m, r) \rangle_{H_{\bar{G}}} = \sum_{k=1}^n \sum_{m=1}^n c_k c_m \bar{G}(r_k, r_m) = \mathbf{c}^\top \bar{\mathbf{G}} \mathbf{c}, \quad (2.16)$$

where $\bar{\mathbf{G}} = \begin{bmatrix} \bar{G}(r_1, r_1) & \cdots & \bar{G}(r_1, r_n) \\ \vdots & \ddots & \vdots \\ \bar{G}(r_n, r_1) & \cdots & \bar{G}(r_n, r_n) \end{bmatrix}$, similar to [30]. Then, the loss (2.6) can be written as:

$$\mathcal{E}_\lambda(\phi) = \mathcal{E}_\infty(\phi) + \lambda \|\phi\|_{H_{\bar{G}}}^2 = \mathbf{c}^\top (\bar{\mathbf{A}} + \lambda \bar{\mathbf{G}}) \mathbf{c} - 2\mathbf{c}^\top \bar{\mathbf{b}} + C_N^f, \quad (2.17)$$

where $\bar{\mathbf{A}}$ and $\bar{\mathbf{b}}$ have the same form as in (2.7) with $\phi_k = \bar{G}(r_k, \cdot)$ and $\phi_{k'} = \bar{G}(r_{k'}, \cdot)$.

2.3 Data-based approximation of the regression and regularization

Given discrete data $\{p_{t_i}(x_j), j = 1, \dots, M\}_{i=1}^N$, we approximate $\bar{\mathbf{A}}$, $\bar{\mathbf{b}}$ and $\bar{\mathbf{G}}$ in (2.17) to compute the estimator. We first write the data as input–output pairs of the nonlocal operator:

$$\mathcal{D} = \left\{ \left(p_{t_i}(x_j), \tilde{f}_{t_i}(x_j) \right), j = 1, \dots, M \right\}_{i=1}^N, \quad (2.18)$$

where the value of $\tilde{f}_{t_i}(x_j)$ is computed via finite difference. That is, for the interior grid points $x_j \in (-L + R_0, L - R_0)$,

$$\tilde{f}_{t_i}(x_j) \doteq \frac{p_{t_{i+1}}(x_j) - p_{t_i}(x_j)}{\Delta t} + \frac{b(x_{j+1})p_{t_i}(x_{j+1}) - b(x_{j-1})p_{t_i}(x_{j-1})}{2\Delta x} - \frac{1}{2} \frac{p_{t_i}(x_{j+1}) - 2p_{t_i}(x_j) + p_{t_i}(x_{j-1}))}{\Delta x^2}. \quad (2.19)$$

For the left/right boundary points, i.e., at $x_j = -L + R_0$ or $x_j = L - R_0$, we approximate the advection term using a three-point forward/backward difference and the diffusion term using a four-point forward/backward difference. Both one-sided schemes for boundary points exhibit $O(\Delta x^2)$ numerical error.

We use Riemann sum to approximate the integrals in the reproducing kernel \bar{G} in (2.10) and in $R_{\bar{G}(r_k, \cdot)}[p_{t_i}](x_j)$. The process starts from piecewise constant approximations of the functions $Q[p_{t_i}](x_j, r)$:

$$\hat{Q}[p_{t_i}](x_j, r) = \sum_{k=1}^n Q[p_{t_i}](x_j, r_k) \mathbf{1}_{I_k}(r), \quad (2.20)$$

for $x_j \in \Omega_{R_0} = [-L + R_0, L - R_0]$. Here, $\{r_k\}$ is a partition of $(0, R_0]$ and are set to be $r_k = k\Delta x, k = 1, 2, \dots, n$ with $n = \lfloor R_0/\Delta x \rfloor$, and $\mathbf{1}_{I_k}(r)$ is the the indicator function for the interval $I_k = ((k-1)\Delta x, k\Delta x]$. Accordingly, the discrete counterpart of the exploration measure ρ in (2.9) and the reproducing kernel $G(r, s)$ in (2.10), denoted by $\hat{\rho}$ and G^M , are given by

$$\begin{aligned} \hat{\rho}(r) &= \frac{1}{ZN} \sum_{i,j,k} |Q[p_{t_i}](x_j, r_k)| \Delta x \mathbf{1}_{I_k}(r), \\ G^M(r, s) &= \frac{\Delta x}{N} \sum_{i=1}^N \sum_{m,\ell,\ell'} Q[p_{t_i}](x_m, r_\ell) Q[p_{t_i}](x_m, s_{\ell'}) \mathbf{1}_{I_\ell}(r) \mathbf{1}_{I_{\ell'}}(s), \end{aligned} \quad (2.21)$$

and the basis function $\phi_k(r) = \bar{G}(r_k, r)$ is

$$\phi_k^M(r) = \bar{G}^M(r_k, r) = \sum_{\ell=1}^n \bar{G}^M(r_k, r_\ell) \mathbf{1}_{I_\ell}(r), \quad \text{with } \bar{G}^M(r, s) = \frac{G^M(r, s)}{\hat{\rho}(r)\hat{\rho}(s)}. \quad (2.22)$$

With the notation $\Phi^M(r) = (\phi_1^M(r), \dots, \phi_n^M(r))^\top$, the estimator $\hat{\phi}_\lambda^{n,M}$ in the finite-dimensional space $H_{\bar{G}^M} = \text{span} \{\phi_k^M\}_{k=1}^n$ admits the representation

$$\hat{\phi}_\lambda^{n,M}(r) = (\hat{\mathbf{c}}_\lambda^{n,M})^\top \Phi^M(r), \quad \hat{\mathbf{c}}_\lambda^{n,M} = (\bar{\mathbf{A}}^M + \lambda \bar{\mathbf{G}}^M)^\dagger \bar{\mathbf{b}}^M. \quad (2.23)$$

Here, $\bar{\mathbf{A}}^M$ and $\bar{\mathbf{b}}^M$ approximate $\bar{\mathbf{A}}$ and $\bar{\mathbf{b}}$ in (2.17) and are given by

$$\bar{\mathbf{A}}^M = \bar{\mathbf{G}}^M \mathbf{G}^M \bar{\mathbf{G}}^M (\Delta x)^2, \quad \bar{\mathbf{b}}^M = \bar{\mathbf{G}}^M \mathbf{Q}^\top \mathbf{f} \Delta x, \quad (2.24)$$

where \mathbf{G}^M , $\bar{\mathbf{G}}^M$, \mathbf{Q} and \mathbf{f} are given by

$$\begin{aligned} \mathbf{Q}_{(i,j),k} &= \sqrt{\frac{\Delta x}{N}} Q[p_{t_i}](x_j, r_k) \in \mathbb{R}^{NM \times n}, & \mathbf{f}_{(i,j)} &= \sqrt{\frac{\Delta x}{N}} \tilde{f}_{t_i}(x_j) \in \mathbb{R}^{NM}, \\ \mathbf{G}^M(k, \ell) &= \sum_{i=1}^N \sum_{j=1}^M \mathbf{Q}_{(i,j),k} \mathbf{Q}_{(i,j),\ell} & \bar{\mathbf{G}}^M(k, \ell) &= \frac{\mathbf{G}^M(k, \ell)}{\hat{\rho}(r_k)\hat{\rho}(r_\ell)} \in \mathbb{R}^{n \times n}. \end{aligned} \quad (2.25)$$

In particular, to improve the numerical stability, instead of using the normal matrix $\bar{\mathbf{A}}^M$, we use the original regression matrix to solve for $\hat{\mathbf{c}}_\lambda^{n,M}$. Specifically, we solve $\hat{\mathbf{c}}_\lambda^{n,M}$ by minimizing

$$\mathcal{E}_\lambda(\mathbf{c}) := \|\mathbf{Q} \bar{\mathbf{G}}^M \mathbf{c}(\Delta r) - \mathbf{f}\|^2 + \lambda \|\mathbf{c}^\top \sqrt{\bar{\mathbf{G}}^M}\|^2, \quad (2.26)$$

which approximates the loss function in (2.17).

3 Convergence of the RKHS-regularized estimator

3.1 Main results

Under suitable smoothness conditions on the true kernel and the data, we show that the regularized RKHS estimator converges as the uniform mesh grid becomes finer.

To ensure that the numerical errors in (2.18) are controlled by Δt and Δx , we strengthen Assumption H1 and impose higher uniform regularity on p_{t_i} and $\partial_t p_t|_{t=t_i}$.

Assumption H1' For each i , the probability density p_{t_i} is supported on $\Omega_{R_0} \subset \mathbb{R}$ such that

$$p_{t_i} \in W^{3,\infty}(\Omega_{R_0}), \quad \partial_t p_t|_{t=t_i} \in W^{1,\infty}(\Omega_{R_0}),$$

with the corresponding $L^\infty(\Omega_{R_0})$ -based Sobolev norms bounded uniformly in i .

Since $Q[p_t](x, 0) = 0$, we have $\rho(0) = 0$. In other words, the data carries no information about $\phi(0)$, so $\phi(0)$ is not identifiable. Thus, we restrict our analysis to $r \in [\delta, R_0]$, where $\rho(r) \geq \rho_0 > 0$, i.e., the exploration measure is uniformly positive over the domain of interest. To further simplify the analysis, we assume that ρ is a positive constant over $[\delta, R_0]$.

Assumption H2 $\rho(r) \equiv \rho_0 > 0$ for $\forall r \in [\delta, R_0]$ with $\delta > 0$.

This assumption enables the next lemma that bridges the discrete matrix formulation of the estimator in (2.24) with a continuous operator formulation, and provides a basis for the convergence analysis in the next section. Its proof is postponed to Appendix A.

Lemma 3.1 (Operator form \Leftrightarrow Matrix form) Under Assumption H2, let $\mathcal{L}_{\bar{G}^M} : L_\rho^2 \rightarrow L_\rho^2$ be the integral operator with kernel \bar{G}^M in (2.21) and $H_{\bar{G}^M} := \text{span}\{\phi_k^M\}_{k=1}^n$ with $\{\phi_k^M\}$ in (2.22). Then, the matrices $\bar{\mathbf{A}}^M$, $\bar{\mathbf{G}}^M$ and vector $\bar{\mathbf{b}}^M$ in (2.24) satisfy

$$\bar{\mathbf{A}}^M(k, k') = \langle \mathcal{L}_{\bar{G}^M} \phi_k^M, \phi_{k'}^M \rangle_{L_\rho^2}, \quad \bar{\mathbf{G}}^M(k, k') = \langle \mathcal{L}_{\bar{G}^M}^{-1} \phi_k^M, \phi_{k'}^M \rangle_{L_\rho^2}, \quad \bar{\mathbf{b}}^M(k) = \langle \phi^{D,M}, \phi_k^M \rangle_{L_\rho^2}.$$

Furthermore, the matrix form estimator in (2.23) has the operator form

$$\hat{\phi}_\lambda^{n,M} = (\mathcal{L}_{\bar{G}^M} + \lambda \mathcal{L}_{\bar{G}^M}^{-1})^{-1} \phi^{D,M} = (\mathcal{L}_{\bar{G}^M}^2 + \lambda I)^{-1} \mathcal{L}_{\bar{G}^M} \phi^{D,M}, \quad (3.1)$$

where $\phi^{D,M}$ is the Riesz representation of the bounded linear functional:

$$\begin{aligned} \langle \phi^{D,M}, \phi \rangle_{L_\rho^2} &= \frac{1}{N} \sum_{i=1}^N \sum_{m=1}^M R_\phi^M[p_{t_i}](x_m) \tilde{f}_{t_i}(x_m) \Delta x, \\ R_\phi^M[p_{t_i}](x) &:= \sum_{\ell=1}^n \int_0^{R_0} Q[p_{t_i}](x, r_\ell) \mathbf{1}_{I_\ell}(r) \phi(r) dr. \end{aligned} \quad (3.2)$$

Moreover, we impose a source condition on the true Lévy density ϕ^* relative to the normal operator $\mathcal{L}_{\bar{G}}$, with β quantifying its smoothness and thereby governing the convergence rates.

Assumption H3 (Source condition) $\phi^* = \mathcal{L}_{\bar{G}}^{\beta/2} w$ for some $\beta \geq 0$, $w \in L_\rho^2$ with $\|w\|_{L_\rho^2} \leq R$.

We assume that the eigenvalues of the normal operator $\mathcal{L}_{\bar{G}}$ decays polynomially. This assumption is supported by the regularity conditions on p_{t_i} in Assumption H1' and Theorem 1.1 in [31], which together imply that $\mathcal{L}_{\bar{G}}$ has polynomial spectral decay.

Assumption H4 (Spectral decay) *There exists $a \geq 0$ and $b > 0$ such that the eigenvalues λ_k of $\mathcal{L}_{\bar{G}}$ in (2.11) satisfy*

$$ak^{-2\varsigma} \leq \lambda_k \leq bk^{-2\varsigma}, \forall k.$$

Here, the polynomial spectral decay exponent ς quantifies the ill-posedness of the inverse problem, and a larger ς indicates a more severe ill-posedness.

We quantify the complexity of the inverse problem at scale λ through a regularized effective dimension. In analogy with classical kernel regression (see, e.g., [32, 33]), but adapted here to the normal operator $\mathcal{L}_{\bar{G}}$ and the DA-RKHS regularization, we define

$$\mathcal{N}(\lambda) := \text{Tr}(\mathcal{L}_{\bar{G}}(\mathcal{L}_{\bar{G}} + \lambda\mathcal{L}_{\bar{G}}^\dagger)^{-1}) = \text{Tr}(\mathcal{L}_{\bar{G}}^2(\mathcal{L}_{\bar{G}}^2 + \lambda I)^{-1}). \quad (3.3)$$

Under Assumption H4, $\mathcal{N}(\lambda)$ grows polynomially as $\lambda \downarrow 0$ with a rate $O(\lambda^{-\frac{1}{4\varsigma}})$ (see Lemma A.4). This quantity will play a central role in the convergence analysis of our RKHS-regularized estimator, stated in Theorem 3.2, by governing the trade-off between approximation and regularization errors as the mesh is refined.

Our main result is the following convergence theorem for the DA-RKHS regularized estimator. The proof is given in Section 3.2.

Theorem 3.2 *Under Assumptions H1', H2 and H3 and with $\mathcal{N}(\lambda)$ in (3.3), for $\varsigma > 1/4$ and $0 < \lambda \leq 1$, the estimator in (2.23) has the error bound*

$$\begin{aligned} \left\| \hat{\phi}_\lambda^{n,M} - \phi^* \right\|_{L_p^2} &\leq C(\beta, C_1) R \lambda^{\min\{\beta/4, 1\}} + C_a(\Delta t + \Delta x + \Delta x^2) \left(\sqrt{\frac{\mathcal{N}(\lambda)}{\lambda}} + \sqrt{\frac{\Delta x}{\lambda^2}} \right) \\ &\quad + C_b \frac{\Delta x}{\lambda} + C_d \frac{\Delta x^2}{\lambda} \sqrt{\frac{\mathcal{N}(\lambda)}{\lambda}} + C_e \frac{\Delta x}{\lambda^{1/2}} + C_f \frac{\Delta x^2}{\lambda^{3/2}} + C_g \frac{\Delta x^{5/2}}{\lambda^2} \end{aligned}$$

with constants $C(\beta, C_1), C_a, C_b, C_c, C_d, C_e, C_f, C_g$ independent of $\lambda, \Delta x, \Delta t$.

Consequently, with $\Delta t \leq \Delta x$ and Assumption H4, taking the optimal regularization hyperparameter $\lambda^* = (\Delta x)^\alpha$ with $\alpha = \frac{1}{\min\{\beta/4, 1\} + 1}$, we have, as $\Delta x \rightarrow 0$,

$$\left\| \hat{\phi}_\lambda^{n,M} - \phi^* \right\|_{L_p^2} \lesssim (\Delta x)^{\alpha \min\{\beta/4, 1\}}, \quad \alpha \min\{\beta/4, 1\} = \begin{cases} \frac{\beta}{\beta+4}, & 0 < \beta \leq 4; \\ \frac{1}{2}, & \beta > 4. \end{cases}$$

The error comes from three sources: the regularization error (the term $O(\lambda^{\min\{\beta/4, 1\}})$), the numerical error and the finite-dimensional RKHS approximation error (the rest terms); see Section 3.2. Here, the numerical error arises from the discretization of the integrals in the normal matrix $\bar{\mathbf{A}}$ and normal vector $\bar{\mathbf{b}}$ in (2.17) via $\bar{\mathbf{A}}^M$ and $\bar{\mathbf{b}}^M$. In particular, the dominating term $O(\Delta x/\lambda)$ comes from the perturbation in $\mathcal{L}_{\bar{G}^M}$ due to the Riemann-sum discretization in x with mesh Δx , which is amplified by the regularized inverse $(\mathcal{L}_{\bar{G}^M}^2 + \lambda I)^{-1}$ with norm bounded by $1/\lambda$. One may reduce this numerical error by using higher-order quadrature rules for the integrals in $\bar{\mathbf{A}}$ and $\bar{\mathbf{b}}$, which would lead to higher-order convergence in Δx . The finite-dimensional RKHS approximation error stems from approximating the infinite-dimensional DA-RKHS $H_{\bar{G}}$ by its finite-dimensional subspace $H_{\bar{G}^n}$, which introduces additional errors of order

$O(\Delta x \sqrt{\frac{\mathcal{N}(\lambda)}{\lambda}} + \frac{\Delta x^{3/2}}{\lambda} + \frac{\Delta x}{\lambda^{1/2}})$. Note that the approximation error and the numerical error are both controlled by the mesh size Δx since the mesh $\Delta r = \Delta x$.

The regularization error decreases as λ decreases, while the numerical and approximation errors increase as λ decreases, which motivates balancing the bias $O(\lambda^{\min\{\beta/4, 1\}})$ against the dominant term $O(\Delta x/\lambda)$ from the numerical error. This balance yields the optimal regularization parameter $\lambda^* \asymp (\Delta x)^{\frac{1}{\min\{\beta/4, 1\}+1}}$ and the convergence rates stated in Theorem 3.2. Notably, when the true kernel is sufficiently smooth with $\beta > 4$, the convergence rate saturates at $O((\Delta x)^{1/2})$, reflecting the limited ability of the RKHS to regularize overly smooth kernels in this inverse problem setting.

Remark 3.3 (Relation to minimax rates) *When the numerical error is negligible when using high-order quadrature, the error bound in Theorem 3.2 would lead to a convergence rate close to the minimax optimal rate for the statistical inverse problems of learning kernels in operators with DA-RKHS regularization in [21] when these rates are adapted to our deterministic setting. Specifically, ignoring the numerical error terms in Theorem 3.2, we have*

$$\left\| \hat{\phi}_\lambda^{n,M} - \phi^* \right\|_{L^2_\rho} \lesssim (\Delta x)^{\alpha \min\{\beta/4, 1\}}, \quad \alpha \min\{\beta/4, 1\} = \begin{cases} \frac{2\beta\zeta}{2\beta\zeta + 4\zeta + 1}, & 0 < \beta \leq 4; \\ \frac{8\zeta}{12\zeta + 1}, & \beta > 4. \end{cases}$$

These rates come from the trade-off between the regularization bias $O(\lambda^{\min\{\beta/4, 1\}})$ and the variance-like term $O\left(\Delta x \sqrt{\frac{\mathcal{N}(\lambda)}{\lambda}}\right) = O(\Delta x \lambda^{-(1+4\zeta)/(8\zeta)})$, which leads to $\lambda^* = O\left((\Delta x)^{\frac{8\zeta}{\min\{\beta/4, 1\}8\zeta + 1 + 4\zeta}}\right)$.

When $\beta \leq 4$, the above rate is close to the minimax rate for $O\left(\left(\frac{1}{\sqrt{M}}\right)^{-\frac{2\beta\zeta}{2\beta\zeta + 2\zeta + 1}}\right)$ with M being the samples size in [21], where the exponent differs slightly due to the different nature of the variance-like term in our deterministic setting compared to the statistical setting there.

Remark 3.4 (Regularity of p_{t_i} and uniform bounds for f_{t_i}) *Under Assumption H1', for each $t_i > 0$ the map $x \mapsto p_{t_i}(x)$ is Lipschitz on Ω_{R_0} with a constant independent of i . In particular, letting $C'_{\max} := \max_{1 \leq i \leq N} \|\partial_x p_{t_i}\|_{L^\infty(\Omega_{R_0})}$, we have*

$$|p_{t_i}(x+u) - p_{t_i}(x)| \leq C'_{\max} |u| \quad \text{for all } x, u \text{ with } x, x+u \in \Omega_{R_0},$$

since $p_{t_i} \in W^{1,\infty}(\Omega_{R_0})$. Moreover, for $f_t(x)$ defined in (2.3), the product rule and Assumption H1' imply that there exist constants $C_0, C_1 < \infty$, independent of i , such that

$$\|f_{t_i}\|_{L^\infty(\Omega_{R_0})} \leq C_0, \quad \|\partial_x f_{t_i}\|_{L^\infty(\Omega_{R_0})} \leq C_1.$$

These constants depend only on $\|b\|_{W^{2,\infty}}$, $\|\sigma^2\|_{W^{3,\infty}}$, and the uniform $W^{3,\infty}$ in x and $W^{1,\infty}$ in t bounds of the densities, but not on the index i .

3.2 Error decomposition and proof of the main theorem

We decompose the estimator's error into three parts: regularization error, approximation error due to a finite-dimensional hypothesis space, and numerical error arising from the use of discrete data to approximate integrals. That is,

$$\left\| \hat{\phi}_\lambda^{n,M}(r) - \phi^*(r) \right\|_{L^2_\rho} \leq \underbrace{\left\| \hat{\phi}_\lambda^{n,M}(r) - \hat{\phi}_\lambda^n(r) \right\|_{L^2_\rho}}_{\text{numerical error}} + \underbrace{\left\| \hat{\phi}_\lambda^n(r) - \phi_\lambda^\infty(r) \right\|_{L^2_\rho}}_{\text{approximation error}} + \underbrace{\left\| \phi_\lambda^\infty(r) - \phi^*(r) \right\|_{L^2_\rho}}_{\text{regularization error}}$$

where the three estimators are defined as

$$\begin{aligned}\phi_\lambda^\infty &:= (\mathcal{L}_{\overline{G}}^2 + \lambda I)^{-1} \mathcal{L}_{\overline{G}}^2 \phi_*, \\ \hat{\phi}_\lambda^n &:= (\mathcal{L}_{\overline{G}^n}^2 + \lambda I)^{-1} \mathcal{L}_{\overline{G}^n} \phi^{D,n}, \\ \hat{\phi}_\lambda^{n,M} &:= (\mathcal{L}_{\overline{G}^M}^2 + \lambda I)^{-1} \mathcal{L}_{\overline{G}^M} \phi^{D,M}.\end{aligned}\tag{3.4}$$

Here, the operator $\mathcal{L}_{\overline{G}^n}$ is the integral operator whose reproducing kernel \overline{G}^n is a piecewise constant approximation of \overline{G} ,

$$\overline{G}^n(r, s) = \sum_{\ell', \ell=1}^n \overline{G}(r_{\ell'}, r_\ell) \mathbf{1}_{I_{\ell'}}(r) \mathbf{1}_{I_\ell}(s), \quad I_l := ((l-1)\Delta r, l\Delta r],\tag{3.5}$$

and the function $\phi^{D,n}$ is the Riesz representation of the bounded linear functional

$$\langle \phi^{D,n}, \phi \rangle_{L_\rho^2} = \frac{1}{N} \sum_{i=1}^N \int R_\phi^n [p_{t_i}](x) f_{t_i}(x) dx, \quad R_\phi^n [p_{t_i}](x) := \sum_{\ell=1}^n \int_\delta^{R_0} Q [p_{t_i}](x, r_\ell) \mathbf{1}_{I_\ell}(r) \phi(r) dr.\tag{3.6}$$

In other words, ϕ_λ^∞ is the regularized estimator in the continuous space $H_{\overline{G}}$; $\hat{\phi}_\lambda^n$ is an estimator in the finite-dimensional RKHS $H_{\overline{G}^n}$ when \overline{G} is approximated by a piecewise constant function \overline{G}^n in r ; and $\hat{\phi}_\lambda^{n,M}$ is the fully discrete regularized estimator based on \overline{G}^M , which is discretized in both r and x .

We bound these errors by the lemmas below, whose proofs are postponed to Appendix A.2.

Lemma 3.5 (Regularization Error) *Under Assumption (H3) on the source and Assumptions H1' which implies the operator bound for $\mathcal{L}_{\overline{G}}$ in Lemma A.1, the regularization error satisfies*

$$\|\phi_\lambda^\infty - \phi^*\|_{L_\rho^2} \leq C(\beta, C_1) R \lambda^{\min\{\beta/4, 1\}},$$

where $C(\beta, C_1) = \left(\frac{\beta}{4}\right)^{\beta/4} \left(1 - \frac{\beta}{4}\right)^{1-\beta/4}$ if $0 < \beta \leq 4$ and $C(\beta, C_1) = C_1^{\frac{\beta}{2}-2}$ if $\beta > 4$.

Lemma 3.6 (Approximation Error) *Under Assumptions (H3) and H2 on the source, for $0 < \lambda \leq 1$, the error between ϕ_λ^∞ and $\hat{\phi}_\lambda^n$ defined (3.4) has a bound*

$$\|\hat{\phi}_\lambda^n - \phi_\lambda^\infty\|_{L_\rho^2} \leq C_L \Delta x \sqrt{\frac{\mathcal{N}(\lambda)}{\lambda}} + C_L \sqrt{2C_1 C_2} \frac{\Delta x^{3/2}}{\lambda} + C_\beta \frac{\Delta x}{\sqrt{\lambda}},$$

where $C_L = 2C_0 \sqrt{C} |\Omega_{R_0}| C'_{\max} \sqrt{\frac{R_0}{\rho_0}}$ and $C_\beta := C_2 C_1^{\beta/2} R + \frac{C_2}{2} C(\beta, C_1) R$.

Lemma 3.7 (Numerical error) *Under Assumption H1' on p_{t_i} , the fully discrete estimator $\hat{\phi}_\lambda^{n,M}$ satisfies, for all $\lambda > 0$,*

$$\begin{aligned}\|\hat{\phi}_\lambda^{n,M} - \hat{\phi}_\lambda^n\|_{L_\rho^2} &\leq \|T_1\|_{L_\rho^2} + \|T_2\|_{L_\rho^2} + \|T_3\|_{L_\rho^2} \\ &\leq K_1 (\Delta t + \Delta x + \Delta x^2) \left(\sqrt{\frac{\mathcal{N}(\lambda)}{\lambda}} + \sqrt{\frac{\Delta x}{\lambda^2}} \right) \\ &\quad + K_2 \frac{\Delta x}{\lambda} + K_3 \frac{\Delta x^2}{\lambda} \sqrt{\frac{\mathcal{N}(\lambda)}{\lambda}} + K_4 \frac{\Delta x^{5/2}}{\lambda^2} + K_5 \frac{\Delta x^2}{\lambda^{3/2}}\end{aligned}$$

Here, constants $K_i > 0$ are independent of Δx , Δt , $\mathcal{N}(\lambda)$ and λ .

Proof of Theorem 3.2. According to Lemma 3.5, Lemma 3.6 and Lemma 3.7, we get

$$\begin{aligned}
\left\| \hat{\phi}_\lambda^{n,M} - \phi^* \right\|_{L_\rho^2} &\leq \left\| \hat{\phi}_\lambda^{n,M} - \hat{\phi}_\lambda^n \right\|_{L_\rho^2} + \left\| \hat{\phi}_\lambda^n - \hat{\phi}_\lambda^\infty \right\|_{L_\rho^2} + \left\| \phi_\lambda^\infty - \phi^* \right\|_{L_\rho^2} \\
&\leq C(\beta, C_1) R \lambda^{\min\{\beta/4, 1\}} + C_L \Delta x \sqrt{\frac{\mathcal{N}(\lambda)}{\lambda}} + C_L \sqrt{2C_1 C_2} \frac{\Delta x^{3/2}}{\lambda} + C_\beta \frac{\Delta x}{\sqrt{\lambda}} \\
&\quad + K_1 (\Delta t + \Delta x + \Delta x^2) \left(\sqrt{\frac{\mathcal{N}(\lambda)}{\lambda}} + \sqrt{\frac{\Delta x}{\lambda^2}} \right) + K_2 \frac{\Delta x}{\lambda} + K_3 \frac{\Delta x^2}{\lambda} \sqrt{\frac{\mathcal{N}(\lambda)}{\lambda}} \\
&\quad + K_4 \frac{\Delta x^{5/2}}{\lambda^2} + K_5 \frac{\Delta x^2}{\lambda^{3/2}}
\end{aligned}$$

By Lemma A.4 and the spectral decay condition H4, the effective dimension exhibits polynomial decay $\mathcal{N}(\lambda) \asymp \lambda^{-1/(4\gamma)}$, so $\sqrt{\frac{\mathcal{N}(\lambda)}{\lambda}} \asymp \lambda^{-\frac{1+4\gamma}{8\gamma}}$. Ignoring constant factors, with sufficiently small mesh Δx and under a suitable Courant-Friedrichs-Lewy condition $\Delta t \leq \Delta x^2$, all higher-order terms in Δx are absorbed into the leading Δx -order contributions and the bound reduces to

$$\left\| \hat{\phi}_\lambda^{n,M} - \phi^* \right\|_{L_\rho^2} \lesssim \lambda^{\min\{\beta/4, 1\}} + \Delta x \lambda^{-\frac{1+4\gamma}{8\gamma}} + \Delta x \lambda^{-1/2} + \Delta x \lambda^{-1}.$$

Since $\gamma > 1/4$, $\{-\frac{1+4\gamma}{8\gamma}, -1/2\} > -1$, so the $\Delta x/\lambda$ term dominates the Δx -dependent contributions. Consequently, the leading trade-off is between the bias and $\Delta x/\lambda$, namely

$$\lambda^{\min\{\beta/4, 1\}} \sim \Delta x \lambda^{-1}$$

Hence, the optimal regularization hyperparameter λ^* has

$$\lambda^* \sim (\Delta x)^\alpha, \quad \text{with } \alpha = \frac{1}{\min\{\beta/4, 1\} + 1} = \begin{cases} \frac{4}{\beta+4}, & 0 < \beta \leq 4 \\ \frac{1}{2}, & \beta > 4 \end{cases}$$

Then we obtain the convergence rate $\left\| \hat{\phi}_\lambda^{n,M} - \phi^* \right\|_{L_\rho^2} \lesssim (\Delta x)^{\alpha \min\{\beta/4, 1\}}$. ■

4 Hyperparameter selection via Bi-level optimization

Selection of the regularization parameter is crucial for obtaining a stable solution for this ill-posed inverse problem. An overly large parameter can cause underfitting, leading to inaccurate solutions, while an excessively small parameter may result in overfitting, producing unstable solutions. While classical methods such as Generalized Cross-Validation (GCV) [25] and the L-curve [24] are widely used, they may suffer from numerical instability [17, 30].

To address these limitations, we investigate a bi-level optimization [23, 34] that selects the hyperparameter by minimizing generalization error on validation data. This approach ensures robust parameter selection and can be easily extended to the simultaneous tuning of multiple hyperparameters. Its ‘‘upper-level’’ selects the hyperparameter by minimizing the validation error, and the ‘‘lower-level’’ solves the regularized regression problem. From (2.26), the bi-level optimization reads:

$$\begin{aligned}
\text{Upper level: } \quad & \gamma_{\text{opt}} = \underset{\gamma}{\operatorname{argmin}} F(\gamma), \quad F(\gamma) := \mathcal{E}(\mathbf{c}(\gamma)) = \|\mathbf{Q}_U \bar{\mathbf{G}} \mathbf{c}(\gamma)(\Delta r) - \mathbf{f}_U\|^2; \\
\text{Lower level: } \quad & \mathbf{c}(\gamma) = \underset{\mathbf{c}}{\operatorname{argmin}} \Psi(\gamma, \mathbf{c}), \quad \Psi(\gamma, \mathbf{c}) := \|\mathbf{Q}_L \bar{\mathbf{G}} \mathbf{c}(\Delta r) - \mathbf{f}_L\|^2 + 10^\gamma \|\mathbf{c}^\top \sqrt{\bar{\mathbf{G}}}\|^2.
\end{aligned} \tag{4.1}$$

Here, we divide the data into a training dataset and a validation dataset by collecting samples at distinct times, and denote them by $(\mathbf{f}_L, \mathbf{Q}_L)$ and $(\mathbf{f}_U, \mathbf{Q}_U)$, respectively. We parameterize λ as $\lambda = 10^\gamma$ to accommodate the typical scale of λ and to optimize over an unconstrained variable. We refer to the outer minimization as the upper-level (UL) problem and the inner minimization as the lower-level (LL) problem.

The lower-level optimization problem is a Tikhonov-regularized least-squares problem. Since $\Psi(\gamma, \mathbf{c})$ is quadratic in \mathbf{c} , it admits the explicit solution

$$\mathbf{c}(\gamma) = [(\Delta r)^\top \bar{\mathbf{G}}^\top \mathbf{Q}_L^\top \mathbf{Q}_L \bar{\mathbf{G}} (\Delta r) + 10^\gamma \bar{\mathbf{G}}]^{-1} \bar{\mathbf{G}} \mathbf{Q}_L^\top \mathbf{f}_L \Delta r. \quad (4.2)$$

For any fixed regularization hyperparameter, it has a unique minimizer.

The upper-level optimization is solved by gradient descent with the update

$$\gamma_{k+1} = \gamma_k - \eta_k \partial_\gamma F(\gamma_k), \quad (4.3)$$

where $\eta_k = \eta/\sqrt{k}$ is the learning rate [35], with η the initial learning rate and k the iteration index. By the chain rule,

$$\partial_\gamma F(\gamma) = (\partial_{\mathbf{c}} \mathcal{E}(\mathbf{c}(\gamma)))^\top \partial_\gamma \mathbf{c}(\gamma). \quad (4.4)$$

Thus, the key task is to evaluate $\partial_\gamma \mathbf{c}(\gamma)$. Existing approaches fall into two classes [36]: (i) explicit gradients, obtained by automatic differentiation through all lower-level iterations, which are memory-intensive; and (ii) implicit gradients, based on the implicit function theorem and the inverse Hessian, typically approximated by a Neumann series [37] or conjugate gradients [38]. In our setting, the inverse Hessian can be expressed in closed form using the generalized singular value decomposition (GSVD) [39], which we already compute to solve the lower-level problem.

For convenience, set

$$\bar{\mathbf{A}}_L \doteq \mathbf{Q}_L \bar{\mathbf{G}} (\Delta r), \quad \bar{\mathbf{A}}_U \doteq \mathbf{Q}_U \bar{\mathbf{G}} (\Delta r), \quad \bar{\mathbf{K}} \doteq \sqrt{\bar{\mathbf{G}}}. \quad (4.5)$$

Then (4.2) can be rewritten as

$$\mathbf{c}(\gamma) = (\bar{\mathbf{A}}_L^\top \bar{\mathbf{A}}_L + 10^\gamma \bar{\mathbf{G}})^{-1} \bar{\mathbf{G}} \mathbf{Q}_L^\top \mathbf{f}_L \Delta r = (\bar{\mathbf{A}}_L^\top \bar{\mathbf{A}}_L + 10^\gamma \bar{\mathbf{K}}^\top \bar{\mathbf{K}})^{-1} \bar{\mathbf{G}} \mathbf{Q}_L^\top \mathbf{f}_L \Delta r. \quad (4.6)$$

Let the GSVD of the pair $(\bar{\mathbf{A}}_L, \bar{\mathbf{K}})$ be

$$\bar{\mathbf{A}}_L = \mathbf{U}_{\bar{\mathbf{A}}_L} \Sigma_{\bar{\mathbf{A}}_L} \mathbf{X}^{-1}, \quad \bar{\mathbf{K}} = \mathbf{V}_{\bar{\mathbf{K}}} \Sigma_{\bar{\mathbf{K}}} \mathbf{X}^{-1},$$

where $\mathbf{U}_{\bar{\mathbf{A}}_L}$ and $\mathbf{V}_{\bar{\mathbf{K}}}$ are orthogonal, \mathbf{X} is invertible, and $\Sigma_{\bar{\mathbf{A}}_L} = \text{diag}(\sigma_i)$, $\Sigma_{\bar{\mathbf{K}}} = \text{diag}(\mu_i)$ satisfy $\sigma_i^2 + \mu_i^2 = 1$. Then the lower-level solution admits the filter-factor representation [39, Eq. (2.19)]

$$\mathbf{c}(\gamma) = \mathbf{X} \sum_{i=1}^n \frac{\sigma_i}{\sigma_i^2 + 10^{2\gamma} \mu_i^2} (\mathbf{u}_i^\top \bar{\mathbf{G}} \mathbf{Q}_L^\top \mathbf{f}_L) e_i \Delta r, \quad (4.7)$$

where \mathbf{u}_i is the i -th column of $\mathbf{U}_{\bar{\mathbf{A}}_L}$ and e_i is the i -th canonical basis vector.

To compute the hypergradient, we apply the implicit function theorem to the lower-level optimality condition and obtain

$$\partial_\gamma \mathbf{c}(\gamma) = -(\nabla_{\mathbf{c}}^2 \Psi(\gamma, \mathbf{c}))^{-1} \partial_{\gamma \mathbf{c}}^2 \Psi(\gamma, \mathbf{c}). \quad (4.8)$$

Combining (4.4) and (4.8) and using the definitions in (4.5) yield

$$\partial_\gamma F(\gamma) = -2 \ln(10) \cdot 10^\gamma (\bar{\mathbf{A}}_U^\top \bar{\mathbf{A}}_U \mathbf{c} - \bar{\mathbf{A}}_U^\top \mathbf{f}_U)^\top (\bar{\mathbf{A}}_L^\top \bar{\mathbf{A}}_L + 10^\gamma \bar{\mathbf{K}}^\top \bar{\mathbf{K}})^{-1} \bar{\mathbf{G}} \mathbf{c}. \quad (4.9)$$

The matrix inverse in (4.9) can be expressed via the GSVD already computed for the lower-level problem. Indeed,

$$(\bar{\mathbf{A}}_L^\top \bar{\mathbf{A}}_L + 10^\gamma \bar{\mathbf{K}}^\top \bar{\mathbf{K}})^{-1} = \mathbf{X} (\Sigma_{\bar{\mathbf{A}}_L}^\top \Sigma_{\bar{\mathbf{A}}_L} + 10^\gamma \Sigma_{\bar{\mathbf{K}}}^\top \Sigma_{\bar{\mathbf{K}}})^{-1} \mathbf{X}^\top, \quad (4.10)$$

where the middle matrix is diagonal, so its inverse is obtained by inverting its diagonal entries. Substituting (4.10) into (4.9) yields the desired gradient for the upper-level update.

To improve numerical stability and convergence speed, we use a momentum scheme with Nesterov acceleration [40] to update γ and apply gradient normalization [41] to mitigate potential gradient explosion. The resulting upper-level update is

$$\gamma_{k+1} = \gamma_k - v_{k+1}, \quad v_{k+1} = \iota v_k + \eta_k \frac{\nabla_\gamma F(\gamma_k - \iota v_k)}{\|\nabla_\gamma F(\gamma_k - \iota v_k)\| + \epsilon}, \quad (4.11)$$

where $F(\gamma)$ is the upper-level objective, k is the iteration index, v_k is the momentum variable with coefficient $\iota \in [0, 1)$, and $d_k = \nabla_\gamma F(\gamma_k - \iota v_k)$ is the look-ahead gradient. Here η_k is the learning rate, $\|\cdot\|$ is the Euclidean norm, and $\epsilon > 0$ ensures numerical stability in the gradient normalization.

We summarize the complete procedure in Algorithm 1 and refer to it as *bilevel-RKHS*.

Algorithm 1: GSVD-based bi-level optimization (bilevel-RKHS)

Input: Sample $\{x_j\}_{j=1}^J$ and $\{(p_{t_i}(x_j), f_{t_i}(x_j)) : j = 1, \dots, J\}_{i=1}^N$.

Initialize: initial learning rate $\eta > 0$, momentum coefficient $\iota \in (0, 1)$, max iterations K , tolerance $\epsilon > 0$; set $v_0 = 0$, $\gamma_0 = 0$

Generate Dataset: Get $(\bar{\mathbf{A}}_L, \bar{\mathbf{A}}_U, \mathbf{f}_U, \mathbf{f}_L, \bar{\mathbf{G}})$ via equation (2.25); set $\bar{\mathbf{K}} = \sqrt{\bar{\mathbf{G}}}$.

$(\mathbf{U}, \mathbf{sm}, \mathbf{X}) = \text{gsvd}(\bar{\mathbf{A}}_L, \bar{\mathbf{K}})$

for $k = 1, \dots, K$: **do**

$$\eta_k = \eta / \sqrt{k}$$

$$\gamma = \gamma_k - \iota v_k$$

Obtain the explicit solution of Lower-Level problem:

$$\mathbf{c}(\gamma) = \text{tikhonov}(\mathbf{U}, \mathbf{sm}, \mathbf{X}, \mathbf{f}_L, 10^\gamma) \text{ with equation (4.7)}$$

Solve the Upper-Level problem with a gradient descent method:

$$v_{k+1} = \iota v_k + \eta_k \frac{\frac{dF}{d\gamma}}{\|\frac{dF}{d\gamma}\| + \epsilon} \text{ using equation (4.9)}$$

$$\gamma_{k+1} = \gamma_k - v_{k+1}$$

end

$$\lambda = 10^{\gamma_{K+1}}, \hat{\mathbf{c}} = \text{tikhonov}(\mathbf{U}, \mathbf{sm}, \mathbf{X}, \mathbf{f}_L, \lambda), \hat{\phi} = \bar{\mathbf{G}} \hat{\mathbf{c}}$$

Output: $\hat{\phi}, \lambda$

In addition, to avoid unnecessary computation, we invoke an early-stopping criterion when updates of the hyperparameter γ become negligible or the loss fails to decrease. Let $\{\gamma\}_{k \geq 1}$ denote the sequence of hyperparameters and $F(\gamma_k)$ the upper-level loss (treated as a validation loss) evaluated on the dataset $(\bar{\mathbf{A}}_U, \mathbf{f}_U, \bar{\mathbf{G}})$. Given thresholds $\varepsilon_\gamma > 0$, $\varepsilon_F > 0$ and a window length

$W \in \mathbb{N}$, define $\Delta\gamma_k := |\gamma_k - \gamma_{k-1}|$ and $\Delta F_k := |F(\gamma_k) - F(\gamma_{k-1})|$ ($k \geq 1$). We stop at the first index

$$K^* := \inf \{k \geq W : \forall t \in \{k - W + 1, \dots, k\}, \Delta\gamma_t < \varepsilon_\gamma \text{ and } \Delta F_t < \varepsilon_F\}.$$

The window length W guards against premature stopping and improves stability.

5 Numerical experiments

In this section, we present numerical experiments to assess the proposed bilevel-RKHS method for estimating the Lévy density from two types of data. The first type is generated by numerical iterative schemes that solve the Fokker-Planck equation, allowing us to validate our method in a controlled setting, since the discretization error of these schemes is explicitly known. The second type is reconstructed from discrete trajectory data via kernel density estimation (KDE), illustrating the applicability of our method to real-world observations. The codes are available at: <https://github.com/senyuanya/bilevel-RKHS-main>.

Performance evaluation: To evaluate performance, we use the upper-level loss and the relative L_ρ^2 error, defined as:

$$\begin{aligned} \text{Loss} &= \|\mathbf{Q}_U \bar{\mathbf{G}} \mathbf{c}(\gamma)(\Delta r) - \mathbf{f}_U\|^2 \\ L_\rho^2 \text{ Error} &= \sqrt{dr \cdot \rho(r) \cdot \left(\hat{\phi}_\lambda^{n,M}(r) - \phi^*(r)\right)^2}. \end{aligned} \quad (5.1)$$

Here, $\hat{\phi}_\lambda^{n,M}$ represents the estimator, while ϕ^* denotes true Lévy density.

We benchmark our approach against existing methods, including the L-curve and GCV, and evaluate different regularization norms within the bilevel framework. First, we compare our RKHS-Bilevel method with RKHS-LC and RKHS-GCV, which select the regularization parameter via the L-curve and generalized cross-validation (GCV), respectively. Second, previous work shows that the RKHS norm outperforms other norms under both L-curve and GCV selection rules [17, 30]. Accordingly, within our bilevel framework, we evaluate regularizers based on the RKHS norm, the L_ρ^2 -norm, and the ℓ^2 -norm. Table 2 summarizes the methods and regularization norms considered when using \bar{G} in (2.15) as the basis function. The numerical experiments also demonstrate convergence with respect to the spatial mesh size, consistent with Theorem 3.2.

Table 2: Methods and Regularization Norms

Methods	Norms	$\ \cdot\ _*^2$
L-curve (LC)	L_ρ^2	$\mathbf{c}^\top \bar{\mathbf{G}} \text{diag}(\boldsymbol{\rho}) \bar{\mathbf{G}}^\top \mathbf{c}$ *
Generalized Cross-Validation (GCV)	ℓ^2	$\mathbf{c}^\top \mathbf{I} \mathbf{c}$ *
Bilevel optimization (Bilevel)	RKHS	$\mathbf{c}^\top \bar{\mathbf{G}} \mathbf{c}$

* We define: $\text{diag}(\boldsymbol{\rho}) = \text{diag}(\Delta r \rho(r_1), \Delta r \rho(r_2), \dots, \Delta r \rho(r_M))$

* Here, \mathbf{I} denotes the identity matrix, and $\|\cdot\|_{\ell^2}$ represents the Euclidean norm.

5.1 Estimation from data consisting of PDE solutions

We first consider the setting in which the data consists of numerical solutions of the Fokker-Planck equation at discrete times. The probability density $p_i^j = p(x_j, t_i)$ is generated by the

finite-difference scheme

$$\begin{aligned} \frac{p_{i+1}^{j+1} - p_i^j}{\Delta t} = & - \frac{b(x_{j+1}) p_i^{j+1} - b(x_{j-1}) p_i^{j-1}}{2\Delta\tilde{x}} + \frac{1}{2} \frac{p_i^{j+1} - 2p_i^j + p_i^{j-1}}{\Delta\tilde{x}^2} \\ & + \sum_{k=0}^M \phi(r_k) (p_i^{j+j_k} + p_i^{j-j_k} - 2p_i^j) \Delta\tilde{r}, \end{aligned} \quad (5.2)$$

with time step $\Delta t = 0.000025$ and spatial steps $\Delta\tilde{x} = \Delta\tilde{r} = 0.005$ chosen to satisfy the CFL condition. We take $\Omega = [-5, 5]$ and $R_0 = 2$, so the nonlocal term is evaluated only for $t \in [0, 1]$ and $x_j \in [-3, 3]$ with $0 \leq j \leq M = R_0/\Delta\tilde{r}$, thereby avoiding truncation error of $p(x, t)$ in the regression. From the resulting numerical solution, we construct the dataset \mathcal{D} in (2.18) on coarser meshes with $\Delta x \in \{0.01, 0.02, 0.025, 0.04\}$. In all experiments we use $N = 30$ uniformly spaced time snapshots. For the bilevel optimization, $N/2$ snapshots are used for training and $N/2$ for validation.

We consider two Lévy measure densities and two drift functions:

- **Lévy Measure Density:** (a) $\phi(|y|) = e^{-|y|^2}$ (b) $\phi(|y|) = e^{-2|y|}$
- **Drift Function:** (a) $b(x) = -0.5x$ (b) $b(x) = \sin x$

The two light-tailed Lévy densities with Gaussian and exponential decay reduce quadrature error when truncating to a compact domain and the globally Lipschitz drifts promote convergence of the scheme and stable numerical differentiation in the Fokker–Planck equation. In our experiments, we optimize using SGD with momentum, using initial learning rates $\eta \in \{0.004, 0.009\}$ with momentum coefficient $\iota = 0.99$ for the linear-drift case and a learning rate $\eta = 0.005$ with momentum coefficient $\iota = 0.95$ for the nonlinear-drift case.

5.1.1 Lévy jump measure with Gaussian decay

Figure 1 and Tables 3–4 show the estimation results for the Gaussian-decay Lévy density $\phi(|y|) = e^{-|y|^2}$ under two drifts: $b(x) = -0.5x$ and $b(x) = \sin x$.

Across both drift settings, Figures 1 and Tables 3–4 show that the RKHS–Bilevel estimator consistently achieves the smallest or near–smallest L_ρ^2 error. In the linear case $b(x) = -0.5x$, RKHS–Bilevel slightly improves on RKHS–GCV and substantially outperforms RKHS–LC, while maintaining stable accuracy as Δx increases. In the nonlinear case $b(x) = \sin x$, RKHS–Bilevel remains accurate and robust, whereas RKHS–GCV becomes noticeably more sensitive to mesh refinement.

The middle panels of Figure 1 and Table 3 confirm that, within the bilevel framework, RKHS–norm regularization is more effective than either L_ρ^2 or ℓ^2 regularization: the RKHS norm yields the lowest relative errors in both drift scenarios.

The right panels of Figure 1 further indicate that, as the outer iterations proceed, the loss, the estimation error, and the hyperparameter γ all converge to stable values, demonstrating reliable convergence of the bilevel optimization procedure.

Table 3: Relative errors of estimators for $\phi(|y|) = e^{-|y|^2}$ under different regularization norms.

Drift term	L_ρ^2 -Bilevel	ℓ^2 -Bilevel	RKHS-Bilevel
$-0.5x$	0.0763	0.1001	0.0045
$\sin x$	0.0100	0.0097	0.0090

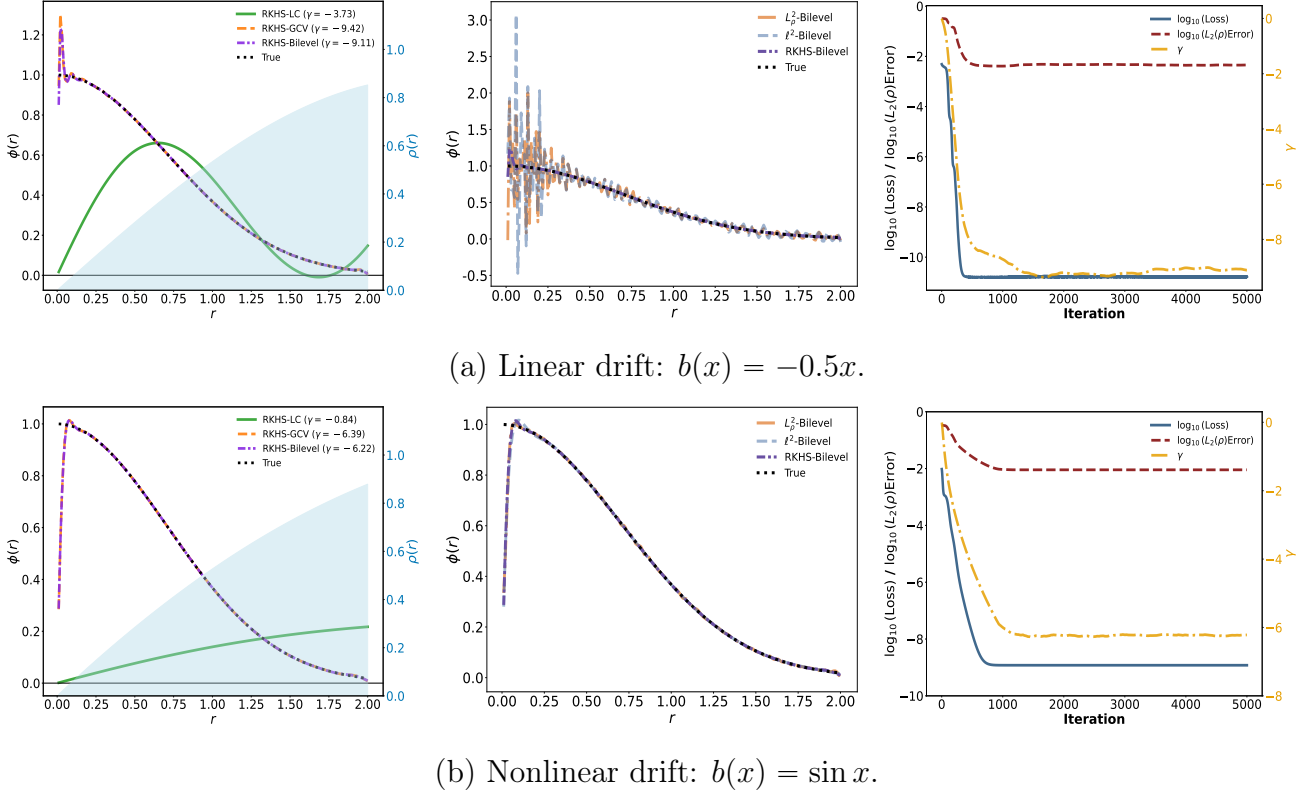


Figure 1: Estimators under linear and nonlinear drift when data with mesh $\Delta x = 0.01$. Left: estimated Lévy density $\phi(|y|) = e^{-|y|^2}$ using different methods; RKHS-Bilevel matches RKHS-GCV and outperforms RKHS-LC. The blue-shaded region indicates the exploration measure ρ . Middle: estimators with different regularization norms, showing RKHS norm is more stable than L_ρ^2 and ℓ^2 . Right: L_ρ^2 error, loss, and γ versus iterations, showing convergence.

Table 4: Relative L_ρ^2 errors for $\phi(|y|) = e^{-|y|^2}$ under $b(x) = -0.5x$ and $b(x) = \sin x$, when the data has varying mesh size Δx . The RKHS-Bilevel method consistently achieves the lowest or near-lowest errors.

Case	Methods	$\Delta x = 0.01$	$\Delta x = 0.02$	$\Delta x = 0.025$	$\Delta x = 0.05$
$b(x) = -0.5x$	RKHS-LC	0.1418	0.1420	0.1416	0.1412
	RKHS-GCV	0.0049	0.0083	0.0215	0.0407
	RKHS-Bilevel	0.0045	0.0212	0.0232	0.0258
$b(x) = \sin x$	RKHS-LC	0.3279	0.0178	0.0210	0.0305
	RKHS-GCV	0.0090	0.0801	0.0962	0.1431
	RKHS-Bilevel	0.0090	0.0197	0.0247	0.0353

5.1.2 Lévy jump measure with Exponential decay

In this subsection, we estimate from data the Lévy density $\phi(|y|) = e^{-2|y|}$ under both a linear drift $b(x) = -0.5x$ and a nonlinear drift $b(x) = \sin x$. Figure 2 shows the estimators for mesh size $\Delta x = 0.01$, while Tables 5 and 6 summarize the relative L_ρ^2 errors for different norms and mesh sizes. In both drift settings, the RKHS-Bilevel estimator is either the best or very close

to the best among all methods: it clearly improves over RKHS–LC and typically matches or slightly outperforms RKHS–GCV, while remaining stable as Δx increases. Within the bilevel framework, RKHS–norm regularization yields the smallest L_ρ^2 errors, outperforming both the L_ρ^2 and ℓ^2 norms, which confirms that the adaptive RKHS is a more suitable function space for this inverse problem. The right column of Figure 2 further shows again that, as iterations proceed, the loss, the L_ρ^2 error, and the hyperparameter γ all converge to steady values, indicating reliable convergence of the bilevel optimization scheme.

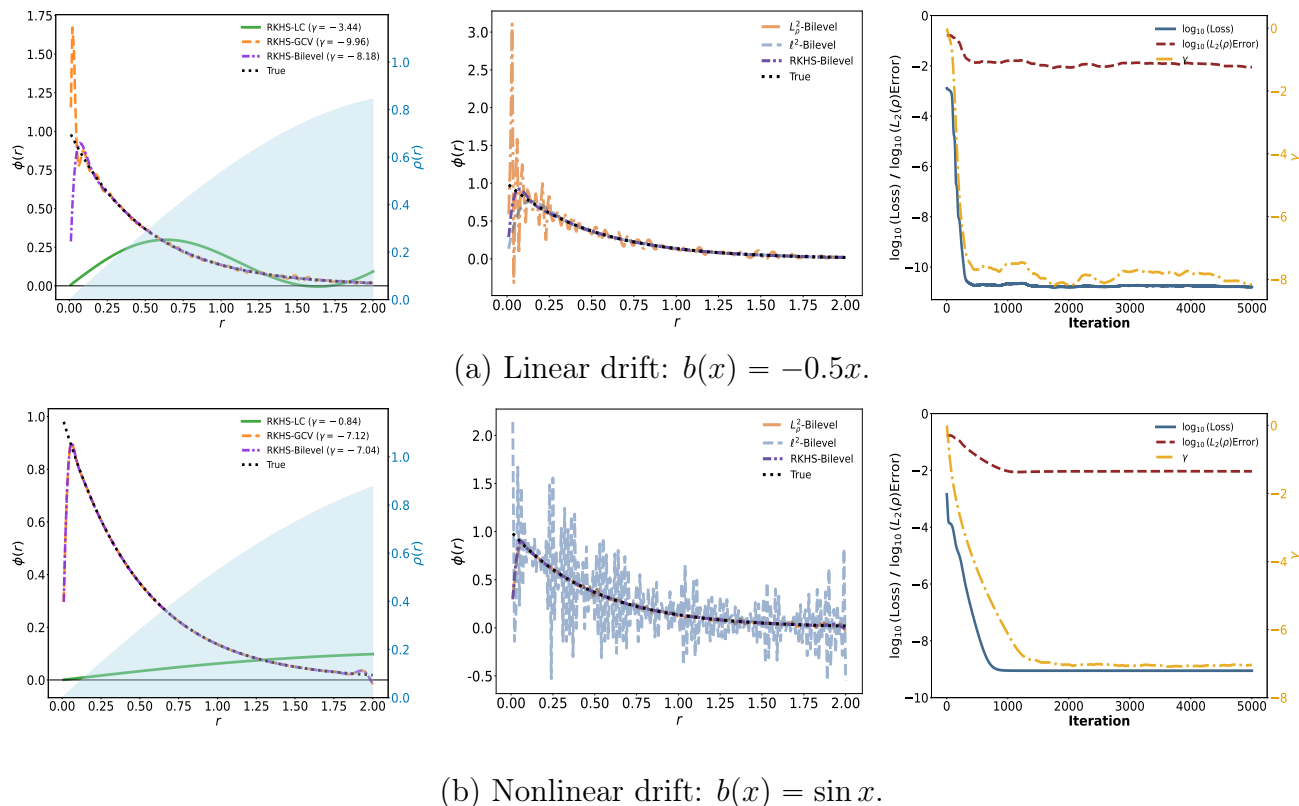


Figure 2: Comparison of estimators under linear and nonlinear drift. Left: estimated Lévy density $\phi(|y|) = e^{-2|y|}$ for different methods. RKHS-Bilevel improves over RKHS–LC and matches or slightly improves upon RKHS–GCV. Blue shading: numerically computed ρ . Middle: effect of regularization norms, with RKHS outperforming L_ρ^2 and ℓ^2 . Right: L_ρ^2 error, loss, and hyperparameter γ over iterations, indicating convergence.

Table 5: Relative errors of estimators for $\phi(|y|) = e^{-2|y|}$ under different regularization norms.

Drift term	L_ρ^2 -Bilevel	ℓ^2 -Bilevel	RKHS-Bilevel
$-0.5x$	0.0564	0.0196	0.0088
$\sin x$	0.0164	0.2856	0.0093

5.1.3 Convergence as the observation mesh size

We next examine the convergence of the regularized estimators as Δx increases; see Fig. 3. On the log–log scale, the L_ρ^2 –error decays with an empirical slope close to 1 in all four test

Table 6: Relative L_ρ^2 errors for $\phi(|y|) = e^{-2|y|}$ under $b(x) = -0.5x$ and $b(x) = \sin x$.

Case	Methods	$\Delta x = 0.01$	$\Delta x = 0.02$	$\Delta x = 0.025$	$\Delta x = 0.05$
$b(x) = -0.5x$	RKHS-LC	0.1088	0.1086	0.1086	0.1082
	RKHS-GCV	0.0136	0.1271	0.0944	0.1623
	RKHS-Bilevel	0.0088	0.0212	0.0220	0.0240
$b(x) = \sin x$	RKHS-LC	0.1700	0.1696	0.1694	0.1688
	RKHS-GCV	0.0095	0.0645	0.0797	0.1230
	RKHS-Bilevel	0.0093	0.0196	0.0248	0.0377

cases. These rates are higher than the rate $(\Delta x)^{1/2}$ in Theorem 3.2, which is proved under the worst-case source condition and only polynomial spectral decay, in the saturated regime $\beta > 4$. This apparent discrepancy is not a contradiction, but reflects that the theorem gives a rate on what can be guaranteed uniformly over all admissible problems, whereas our examples are much smoother than required by the theory (i.e., ϕ^* is smooth, corresponding to $\beta = \infty$). In particular, the densities $\{p_{t_i}\}$ are smooth and dependent, so the normal matrix has multiple zero eigenvalues, not satisfying the polynomial spectral decay condition. In this setting, the bilevel choice of λ drives the solution into a regime where the dominant contribution to the error comes from discretization (finite differences in x and the piecewise-constant approximation in r), which is first-order in Δx . Hence, the observed L_ρ^2 -error behaves like $O(\Delta x)$, i.e., with slope close to 1.

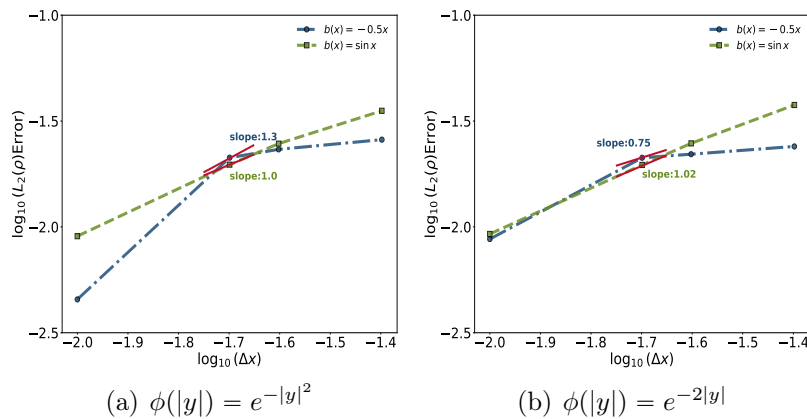


Figure 3: Convergence of estimator error and loss as mesh refines. The L_ρ^2 error decays approximately like $O(\Delta x)$ (slope close to 1), faster than the worst-case theoretical rate, due to high smoothness of data in the examples.

5.2 Lévy density estimation from a sequence of ensembles

Another practical scenario is to estimate the Lévy density ϕ directly from a sequence of sample ensembles of the underlying SDE, without access to the density data. In this setting, we first estimate the densities p_{t_i} from the ensemble data using kernel density estimation (KDE) and then use the estimated densities to construct the dataset \mathcal{D} in (2.18).

Following [6], we consider the simplest setting of estimating the Lévy density ϕ of the Lévy

process L_t :

$$dX_t = dL_t, \quad (5.3)$$

from data consisting of sequence of ensembles $\{\mathcal{S}_i\}_{i=1}^N$ with $\mathcal{S}_i = \left\{ X_{t_i}^{(j)} \right\}_{j=1}^J$, where $X_{t_i}^{(j)}$ is the j -th sample at time t_i .

We generate the data using the Euler–Maruyama scheme. A key step is to compute the increment $\Delta L_{t_i} = L_{t_{i+1}} - L_{t_i}$, where the driving Lévy process is taken to be compound Poisson. By [42][Theorem 3.1], we simulate these increments in two steps: (i) compute the jump arrival rate $\lambda = \int_{\mathbb{R} \setminus \{0\}} \nu(dy)$, and the distribution of jump $\frac{\nu(dy)}{\lambda}$; (ii) simulate the compound Poisson process L_t of the form $L_t := \sum_{i=1}^{\infty} V^i 1_{[t \geq T_i]}$, where T_i are Poisson arrival times of intensity λ and V_i are i.i.d. with law $\mu := (1/\lambda)\nu$.

Numerical settings: To obtain discrete observations $\{\mathcal{S}_i\}_{i=1}^N$, we simulate $J = 10^6$ trajectories over $t \in [0, 5]$ with time step $\Delta t = 0.05$ via the explicit Euler scheme. The Lévy increments are constructed in accordance with the two types of Lévy densities introduced in Subsection 5.1:

- (a) **Gaussian decay:** $\phi(|y|) = e^{-|y|^2}$; $\lambda = \sqrt{\pi}$; $\mu(y) = \frac{e^{-|y|^2}}{\sqrt{\pi}}$; $V_i \sim \mathcal{N}(0, \frac{1}{2})$
- (b) **Exponential decay:** $\phi(|y|) = e^{-2|y|}$; $\lambda = 1$; $\mu(y) = e^{-2|y|}$; $V_i \sim \text{Laplace}(0, \frac{1}{2})$.

From the ensemble data, we estimate the density $p(\cdot, t_i)$ at each time point t_i using KDE. For each t_i , we evaluate the KDE on a uniform grid $x_k \in [-5, 5]$ with spacing $\Delta x = 0.01$. To stabilize numerical differentiation, we smooth the KDE values with a Savitzky–Golay (SG) filter [43] and then apply finite differences to the smoothed PDF, thereby constructing dataset \mathcal{D} in (2.18). Unless otherwise specified, we use a KDE bandwidth $h = 0.105$, corresponding to $c = 0.5$ in the rule $h = c(J\Delta t^2)^{-1/5}$.

For the bilevel optimization, we fix $\eta = 0.005$ and $\iota = 0.85$ in our algorithm.

Figure 4 summarizes the estimators obtained from ensemble data for both Lévy densities, $\phi(|y|) = e^{-|y|^2}$ and $\phi(|y|) = e^{-2|y|}$. In each case, the RKHS–Bilevel method produces the visually best fit, while RKHS–LC is slightly less accurate and RKHS–GCV can become unstable (in particular for the exponential-decay density, where the GCV curve is highly oscillatory). The right panels show that, for both densities, the loss, the L_ρ^2 error and the hyperparameter γ converge as the outer iterations proceed.

Table 7 reports the corresponding L_ρ^2 errors. They confirm that RKHS–Bilevel attains the smallest error among the three hyperparameter–selection methods, and also compare bilevel optimization under different regularization norms. Across both densities, RKHS–norm regularization clearly outperforms L_ρ^2 –Bilevel (which is very unstable) and ℓ^2 –Bilevel (which yields larger errors), reinforcing the advantage of the adaptive RKHS norm in this setting.

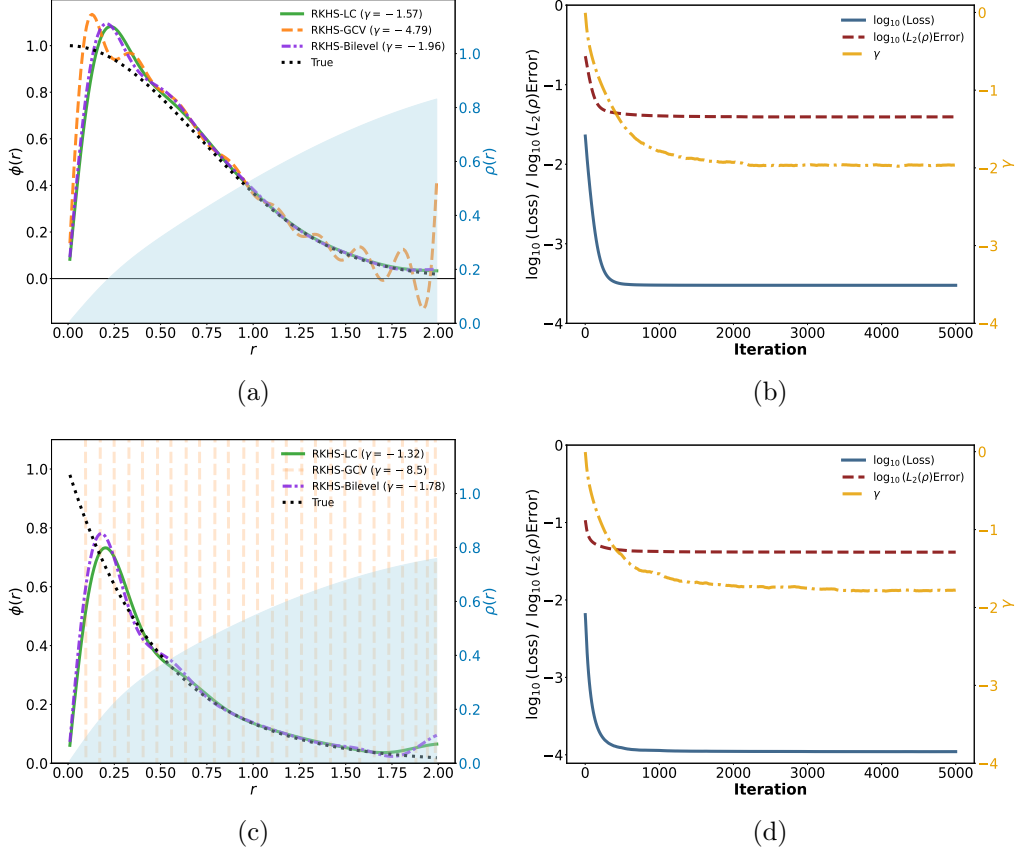


Figure 4: Estimators from ensemble data. (a) & (c): Regularized estimators with hyperparameter selected by L-curve, GCV and bi-level methods. RKHS-Bilevel outperforms RKHS-GCV and slightly improves upon RKHS-LC. (b)& (d): Decay of the L_ρ^2 error, loss, and regularization hyperparameter γ over iterations, illustrating the convergence behavior of RKHS-Bilevel.

Table 7: Relative L_ρ^2 errors across methods and norms for two Lévy densities

ϕ	Different methods		Different norms	
	Setting	Error	Setting	Error
$e^{- y ^2}$	RKHS-LC	0.0421	L_ρ^2 -Bilevel	5.3434
	RKHS-GCV	0.0687	ℓ^2 -Bilevel	0.0460
	RKHS-Bilevel	0.0394		
$e^{-2 y }$	RKHS-LC	0.0442	L_ρ^2 -Bilevel	55.2078
	RKHS-GCV	11.9383	ℓ^2 -Bilevel	0.0479
	RKHS-Bilevel	0.0414		

Figure 5 illustrates the impact of the KDE bandwidth h (parameterized by c in the formula $h = c(J\Delta t^2)^{-1/5}$) on both the estimated PDFs and the recovered Lévy densities. In panels (a) and (c), smaller bandwidths yield less-smoothed, more oscillatory KDEs, while larger bandwidths produce smoother but more biased density estimates, especially near the origin. Panels (b) and

(d) show the corresponding Lévy density estimates: when h is too small the estimates inherit strong oscillations from the noisy PDFs, whereas for overly large h the estimates become overly smooth and lose accuracy. These results highlight the crucial role of choosing an appropriate bandwidth: it must be small enough to preserve the structure of p_t for accurate recovery of ϕ , yet large enough to stabilize numerical differentiation and suppress spurious oscillations.

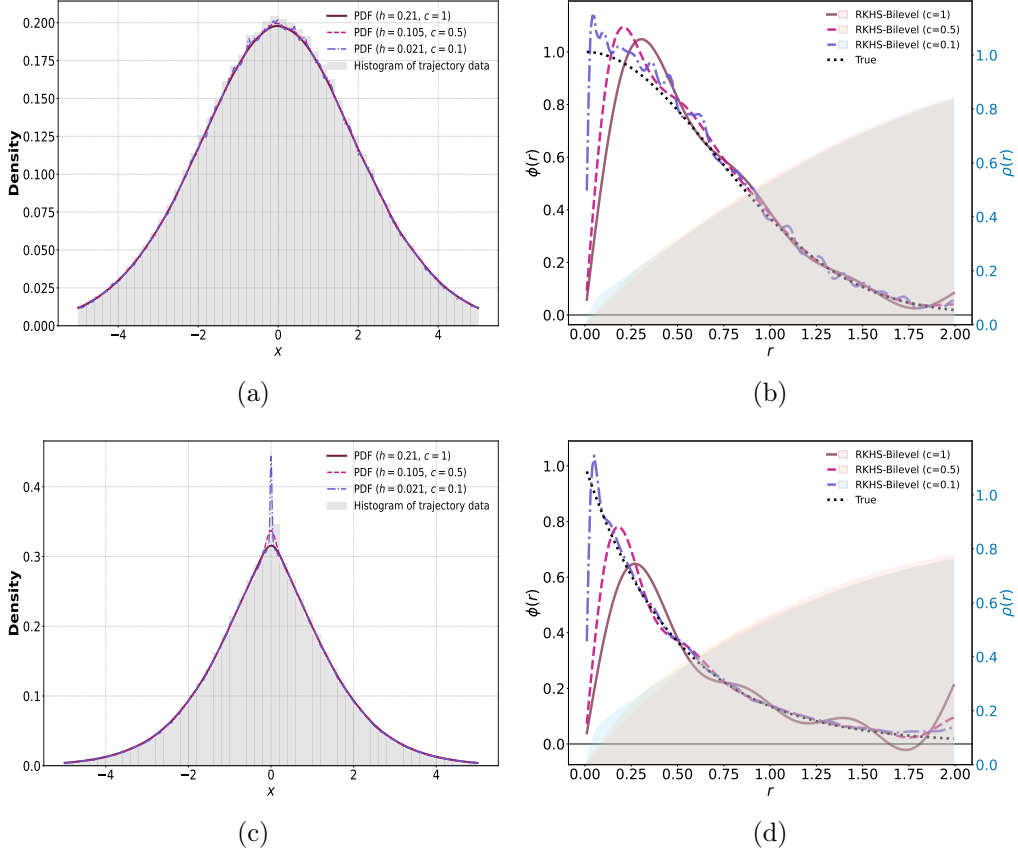


Figure 5: Effect of the KDE bandwidth on density and Lévy-density estimation for both Gaussian- and exponential-decay Lévy measures. (a,c): KDE approximations of the PDF at a fixed time for several bandwidths h (encoded by the constant c). Smaller h produces more oscillatory PDFs; larger h yields smoother but more biased PDFs near the origin. (b,d): corresponding Lévy-density estimates: smaller h leads to oscillatory estimates, while larger h gives smoother but less accurate recovery.

6 Conclusion

We developed a nonparametric framework for learning the Lévy density ϕ in the Fokker-Planck equation using an adaptive RKHS and bilevel optimization. Our main theoretical result is a mesh-dependent error bound for the DA-RKHS Tikhonov estimator. Under a power spectral decay condition on the normal operator, we proved that the reconstruction error decays in the spatial mesh size, with an optimal choice of the regularization parameter balancing regularization bias and numerical/approximation errors. When numerical errors are negligible, the resulting rates are comparable to minimax-optimal rates for inverse statistical learning, while making explicit how spatial discretization degrades accuracy.

Algorithmically, we proposed a GSVD-based bilevel scheme (*bilevel-RKHS*) to select the regularization parameter by minimizing a validation loss. The lower level solves the Tikhonov problem in closed form via GSVD, and the same decomposition provides an explicit inverse-Hessian for efficient hypergradient computation in the upper level.

Numerically, we demonstrated that the bilevel-RKHS method yields more accurate and stable Lévy density estimates than L-curve and GCV across multiple Lévy densities and drift fields. Also, the adaptive RKHS norm outperforms L_ρ^2 - and ℓ^2 -based regularizers within the same bilevel framework.

Acknowledge

L. Yang is partially supported by the CSC Fellowship, and would like to thank Prof. Xin Tong and Prof. Haibo Li for helpful discussions. The work of F.Lu is partially supported by the National Science Foundation under grant DMS-2238486 and DMS-2511283. This work of J. Duan and T. Gao was supported in part by the National Natural Science Foundation of China (12401233 and 12141107), the NSFC International Collaboration Fund for Creative Research Teams (Grant W2541005), the National Key Research and Development Program of China (2021ZD0201300), Guangdong Provincial Key Laboratory of Mathematical and Neural Dynamical Systems (2024B1212010004), the Guangdong Basic and Applied Basic Research Foundation (2025A1515011645), the Guangdong-Dongguan Joint Research Fund (2023A1515140016), the Cross Disciplinary Research Team on Data Science and Intelligent Medicine (2023KCXTD054).

A Appendix: technical results and proofs

A.1 Proof of lemmas on RKHS

Proof of Lemma 2.1. By definition, \bar{G} is positive semi-definite, i.e., for any finite set of points $\{r_i\}_{i=1}^m \subset \mathbb{R}^1$ and any coefficients $c_1, c_2, \dots, c_m \in \mathbb{R}$, we have $\sum_{k=1}^n c_k \sum_{k=1}^m c_k \bar{G}(r_j, r_k) \geq 0$.

To show $\bar{G} \in L^2(\rho \otimes \rho)$, note that by Assumption H1,

$$\max_i \sup_{x \in \Omega, r \in [0, R_0]} |Q[p_{t_i}](x, r)| \leq 4 \max_i \sup_{x \in \Omega} p_{t_i}(x) \leq 4C_{max}.$$

Then, for any $r, s \in [0, R_0]$, we have

$$\begin{aligned} G(r, s) &= \frac{1}{N} \sum_{i=1}^N \int (Q[p_{t_i}](x, r) Q[p_{t_i}](x, s)) dx \\ &\leq 4C_{max} \frac{1}{N} \sum_{i=1}^N \int |Q[p_{t_i}](x, r)| dx \leq 4C_{max} Z \rho(r). \end{aligned} \tag{A.1}$$

Then, by the symmetry of \bar{G} , we obtain

$$\iint |\bar{G}(r, s)|^2 \rho(r) \rho(s) dr ds = \iint \left| \frac{G(r, s)}{\rho(r) \rho(s)} \right|^2 \rho(r) \rho(s) dr ds \leq 16C_{max}^2 Z^2 < \infty. \tag{A.2}$$

That is, $\bar{G} \in L^2(\rho \otimes \rho)$.

To prove (2.12), by definition of $\mathcal{L}_{\overline{G}}$ in (2.11), we have

$$\begin{aligned}\langle \mathcal{L}_{\overline{G}}\phi, \psi \rangle_{L^2_\rho} &= \frac{1}{N} \sum_{i=1}^N \int_{\Omega_{R_0}} R_\phi [p_{t_i}] R_\psi [p_{t_i}] dx \\ &= \frac{1}{N} \sum_{i=1}^N \int_{\Omega_{R_0}} \left(\int_0^{R_0} \phi(r) Q[p_{t_i}](x, r) dr \int_0^{R_0} \psi(s) Q[p_{t_i}](x, s) ds \right) dx \\ &= \int_0^{R_0} \int_0^{R_0} \phi(r) \psi(s) G(r, s) dr ds = \int_0^{R_0} \int_0^{R_0} \phi(r) \psi(s) \overline{G}(r, s) \rho(dr) \rho(ds).\end{aligned}$$

Then, the loss function can be written as

$$\mathcal{E}_\infty(\phi) = \frac{1}{N} \sum_{i=1}^N \int_{\Omega_{R_0}} |R_\phi [p_{t_i}](x) - f_{t_i}(x)|^2 dx = \langle \mathcal{L}_{\overline{G}}\phi, \phi \rangle_{L^2_\rho} - 2\langle \phi^D, \phi \rangle_{L^2_\rho} + C.$$

Its Fréchet derivative in L^2_ρ is $\nabla \mathcal{E}(\phi) = 2(\mathcal{L}_{\overline{G}}\phi - \phi^D)$. Thus, its unique minimizer in $\text{Null}(\mathcal{L}_{\overline{G}})^\perp$ is $\hat{\phi} = \mathcal{L}_{\overline{G}}^{-1}\phi^D$. ■

Proof of Lemma 3.1 (Operator form \Leftrightarrow Matrix form). Since $\mathcal{L}_{\overline{G}^M}$ is defined by $(\mathcal{L}_{\overline{G}^M}\phi)(r) = \int_0^{R_0} \overline{G}^M(r, s) \phi(s) \rho(s) ds$, using the definition of G^M in (2.21) and \overline{G}^M in (2.22) and interchanging sums and integrals yields

$$\overline{\mathbf{A}}^M(k, k') = \int_0^{R_0} \int_0^{R_0} G^M(r, s) \phi_k^M(r) \phi_{k'}^M(s) dr ds = \langle \mathcal{L}_{\overline{G}^M}\phi_k^M, \phi_{k'}^M \rangle_{L^2_\rho}.$$

The reproducing property of \overline{G}^M implies that

$$\overline{\mathbf{G}}^M(k, k') = \overline{G}^M(r_k, r_{k'}) = \langle \phi_k^M, \phi_{k'}^M \rangle_{H_{\overline{G}^M}} = \langle \mathcal{L}_{\overline{G}^M}^{-1}\phi_k^M, \phi_{k'}^M \rangle_{L^2_\rho}.$$

The identity $\overline{\mathbf{b}}^M(k) = \langle \phi^{D, M}, \phi_k^M \rangle_{L^2_\rho}$ follows from the definition of $\phi^{D, M}$ and $R_{\phi_k^M}^M$ in (3.2).

Operator form \Rightarrow Matrix form The operator form in (3.1) is equivalent to

$$(\mathcal{L}_{\overline{G}^M} + \lambda \mathcal{L}_{\overline{G}^M}^{-1}) \hat{\phi}_\lambda^{n, M} = \phi^{D, M}.$$

Expand $\hat{\phi}_\lambda^{n, M} = \sum_{j=1}^n c_j \phi_j^M$ and test against each basis function ϕ_k^M :

$$\sum_j c_j \langle \mathcal{L}_{\overline{G}^M}\phi_j^M, \phi_k^M \rangle_{L^2_\rho} + \lambda \sum_j c_j \langle \mathcal{L}_{\overline{G}^M}^{-1}\phi_j^M, \phi_k^M \rangle_{L^2_\rho} = \langle \phi^{D, M}, \phi_k^M \rangle_{L^2_\rho}.$$

In matrix form, this is $(\overline{\mathbf{A}}^M + \lambda \overline{\mathbf{G}}^M)\mathbf{c} = \overline{\mathbf{b}}^M$. Thus, the solution is $\hat{\mathbf{c}}_\lambda^{n, M} = (\overline{\mathbf{A}}^M + \lambda \overline{\mathbf{G}}^M)^{-1} \overline{\mathbf{b}}^M$. *Matrix form \Rightarrow operator form.* Conversely, suppose $\hat{\phi}_\lambda^{n, M} = \sum_j \hat{c}_j \phi_j^M$ with $\hat{\mathbf{c}}_\lambda^{n, M}$ solving $(\overline{\mathbf{A}}^M + \lambda \overline{\mathbf{G}}^M)\hat{\mathbf{c}}_\lambda^{n, M} = \overline{\mathbf{b}}^M$. Then for each k ,

$$\sum_j \hat{c}_j \langle \mathcal{L}_{\overline{G}^M}\phi_j^M, \phi_k^M \rangle_{L^2_\rho} + \lambda \sum_j \hat{c}_j \langle \mathcal{L}_{\overline{G}^M}^{-1}\phi_j^M, \phi_k^M \rangle_{L^2_\rho} = \langle \phi^{D, M}, \phi_k^M \rangle_{L^2_\rho}.$$

Since $\{\phi_k^M\}$ spans $H_{\overline{G}^M}$, this implies

$$\langle \mathcal{L}_{\overline{G}^M}\hat{\phi}_\lambda^{n, M} + \lambda \mathcal{L}_{\overline{G}^M}^{-1}\hat{\phi}_\lambda^{n, M} - \phi^{D, M}, \psi \rangle_{L^2_\rho} = 0 \quad \forall \psi \in H_{\overline{G}^M}.$$

Since $\mathcal{L}_{\bar{G}^M}(L_\rho^2) \subset H_{\bar{G}^M}$ and $\mathcal{L}_{\bar{G}^M}$ is self-adjoint, replacing the test function ψ by $\mathcal{L}_{\bar{G}^M}\phi$ with $\phi \in L_\rho^2$, we obtain

$$\langle (\mathcal{L}_{\bar{G}^M}^2 + \lambda I)\hat{\phi}_\lambda^{n,M} - \mathcal{L}_{\bar{G}^M}\phi^{D,M}, \phi \rangle_{L_\rho^2} = 0 \quad \forall \phi \in L_\rho^2,$$

i.e., $(\mathcal{L}_{\bar{G}^M}^2 + \lambda I)\hat{\phi}_\lambda^{n,M} = \mathcal{L}_{\bar{G}^M}\phi^{D,M}$, or equivalently, the operator form in (3.1). ■

A.2 Proofs of three key Lemmas

In this subsection we prove three key lemmas used in the proof of Theorem 3.2.

Proof of Lemma 3.5 (Regularization Error). Note that

$$\phi_\lambda^\infty - \phi^* = (\mathcal{L}_{\bar{G}}^2 + \lambda I)^{-1} \mathcal{L}_{\bar{G}}^2 \phi^* - \phi^* = -\lambda (\mathcal{L}_{\bar{G}}^2 + \lambda I)^{-1} \phi^*. \quad (\text{A.3})$$

Since $\phi^* = \mathcal{L}_{\bar{G}}^{\beta/2} w$ with $w \in L_\rho^2$ and $\mathcal{L}_{\bar{G}}$ is compact, by spectral representation we obtain,

$$\|\phi_\lambda^\infty - \phi^*\|_{L_\rho^2} \leq \sup_{t \in \sigma(\mathcal{L}_{\bar{G}}^2)} \frac{\lambda t^{\beta/4}}{t + \lambda} \|w\|_{L_\rho^2}.$$

Since $\|\mathcal{L}_{\bar{G}}\| \leq C_1$ by Lemma A.1, we have $\sigma(\mathcal{L}_{\bar{G}}^2) \subset [0, C_1^2]$. Set $h_\lambda(t) := \lambda t^{\beta/4}/(t + \lambda)$. Write $t = \lambda s$ to get $h_\lambda(\lambda s) = \lambda^{\beta/4} \frac{s^{\beta/4}}{1+s}$.

- If $0 < \beta < 4$, the function $s^\alpha/(1+s)$ with $\alpha := \beta/4 \in (0, 1)$ attains its maximum at $s = \alpha/(1-\alpha)$ with value $\alpha^\alpha(1-\alpha)^{1-\alpha}$. Hence $\sup_{t \geq 0} h_\lambda(t) = (\frac{\beta}{4})^{\beta/4} (1 - \frac{\beta}{4})^{1-\beta/4} \lambda^{\beta/4}$.
- If $\beta = 4$, $h_\lambda(t) = \lambda t/(t + \lambda) \leq \lambda$.
- If $\beta > 4$, $h_\lambda(t) \leq \lambda t^{\beta/4-1} \leq \lambda C_1^{\beta/2-2}$.

Combine these and $\|w\|_{L_\rho^2} \leq R$ to obtain the stated bound. ■

Proof of Lemma 3.6 (Approximation Error). Recall that $\phi_\lambda^\infty = (\mathcal{L}_{\bar{G}}^2 + \lambda I)^{-1} \mathcal{L}_{\bar{G}}\phi^D$, $\hat{\phi}_\lambda^n = (\mathcal{L}_{\bar{G}^n}^2 + \lambda I)^{-1} \mathcal{L}_{\bar{G}^n}\phi^{D,n}$. Fix $\lambda > 0$, denoting

$$\mathcal{A} := \mathcal{L}_{\bar{G}}^2 + \lambda I, \mathcal{A}_n := \mathcal{L}_{\bar{G}^n}^2 + \lambda I,$$

and using the resolvent identity $(\mathcal{A}_n)^{-1} - \mathcal{A}^{-1} = (\mathcal{A}_n)^{-1}(\mathcal{A} - \mathcal{A}_n)\mathcal{A}^{-1}$, we have

$$\begin{aligned} \hat{\phi}_\lambda^n - \phi_\lambda^\infty &= (\mathcal{A}_n)^{-1} \mathcal{L}_{\bar{G}^n} (\phi^{D,n} - \phi^D) + (\mathcal{A}_n)^{-1} (\mathcal{L}_{\bar{G}^n} - \mathcal{L}_{\bar{G}}) \phi^D + (\mathcal{A}_n)^{-1} (\mathcal{A} - \mathcal{A}_n) \mathcal{A}^{-1} \mathcal{L}_{\bar{G}} \phi^D \\ &= (\mathcal{A}_n)^{-1} \mathcal{L}_{\bar{G}^n} (\phi^{D,n} - \phi^D) + (\mathcal{A}_n)^{-1} (\mathcal{L}_{\bar{G}^n} - \mathcal{L}_{\bar{G}}) \phi^D + (\mathcal{A}_n)^{-1} (\mathcal{A} - \mathcal{A}_n) \phi_\lambda^\infty. \end{aligned} \quad (\text{A.4})$$

We first bound $\|(\mathcal{A}_n)^{-1} \mathcal{L}_{\bar{G}^n} (\phi^{D,n} - \phi^D)\|_{L_\rho^2}$. Recall the definitions of $\phi^{D,n}$ and ϕ^D in (3.6) and (2.13), we have, for any $\phi \in L_\rho^2$,

$$\begin{aligned} \left| \langle \phi^{D,n} - \phi^D, \phi \rangle_{L_\rho^2} \right| &= \left| \int_\delta^{R_0} \int \left(\sum_{\ell=1}^n Q(x, r_\ell) \mathbf{1}_{I_\ell}(r) - Q(x, r) \right) \phi(r) dr f_{t_i}(x) dx \right| \\ &\leq \|f_{t_i}\|_\infty |\Omega_{R_0}| \sup_x \sum_\ell \int_{I_\ell} |Q(x, r_\ell) - Q(x, r)| |\phi(r)| dr \\ &\leq 2C_0 |\Omega_{R_0}| C'_{\max} \Delta r \int_\delta^{R_0} |\phi(r)| dr \leq 2C_0 |\Omega_{R_0}| C'_{\max} \Delta r \sqrt{\frac{R_0}{\rho_0}} \|\phi\|_{L_\rho^2}. \end{aligned}$$

Here, under Assumption H2, we get $\rho(r) = \rho_0$. Therefore, since $\Delta r = \Delta x$, we have

$$\|\phi^{D,n} - \phi^D\|_{L^2_\rho} = \sup_{\|\phi\|_{L^2_\rho}=1} |\langle \phi^{D,n} - \phi^D, \phi \rangle| \leq 2C_0 |\Omega_{R_0}| C'_{\max} \sqrt{\frac{R_0}{\rho_0}} \Delta x.$$

Meanwhile, Lemma A.2 gives $\|\mathcal{A}_n^{-1} \mathcal{L}_{\bar{G}^n} \phi\|_{L^2_\rho} \leq \sqrt{\frac{\mathcal{N}_n(\lambda)}{\lambda}} \|\phi\|_{L^2_\rho}$ for any $\phi \in L^2_\rho$, and Lemma A.3 implies $|\mathcal{N}_n(\lambda) - \mathcal{N}(\lambda)| \leq \frac{2C_1 C_2}{\lambda} \Delta x$. Thus, $\mathcal{N}_n(\lambda) \leq \mathcal{N}(\lambda) + |\mathcal{N}_n(\lambda) - \mathcal{N}(\lambda)|$ and $\sqrt{a+b} \leq \sqrt{a} + \sqrt{b}$ imply

$$\sqrt{\frac{\mathcal{N}_n(\lambda)}{\lambda}} \leq \sqrt{\frac{\mathcal{N}(\lambda)}{\lambda}} + \sqrt{\frac{2C_1 C_2}{\lambda^2}} \Delta x. \quad (\text{A.5})$$

Cobming the above estimates with notation $C_L := 2C_0 |\Omega_{R_0}| C'_{\max} \sqrt{\frac{R_0}{\rho_0}}$, we obtain,

$$\begin{aligned} \|\mathcal{A}_n^{-1} \mathcal{L}_{\bar{G}^n} (\phi^{D,n} - \phi^D)\|_{L^2_\rho} &\leq \sqrt{\frac{\mathcal{N}_n(\lambda)}{\lambda}} \|\phi^{D,n} - \phi^D\|_{L^2_\rho} \\ &\leq C_L \Delta x \sqrt{\frac{\mathcal{N}(\lambda)}{\lambda}} + C_L \sqrt{2C_1 C_2} \frac{\Delta x^{3/2}}{\lambda}. \end{aligned}$$

Next, to bound the last two terms in (A.4), observe that

$$\mathcal{A}_n^{-1} (\mathcal{L}_{\bar{G}^n} - \mathcal{L}_{\bar{G}}) \phi^D + \mathcal{A}_n^{-1} (\mathcal{A} - \mathcal{A}_n) \phi_\lambda^\infty = \mathcal{A}_n^{-1} \mathcal{L}_{\bar{G}^n} (\mathcal{L}_{\bar{G}} - \mathcal{L}_{\bar{G}^n}) \phi^* + \mathcal{A}_n^{-1} (\mathcal{L}_{\bar{G}^n}^2 - \mathcal{L}_{\bar{G}}^2) (\phi^* - \phi_\lambda^\infty).$$

Using $\|\mathcal{L}_{\bar{G}^n} - \mathcal{L}_{\bar{G}}\| \leq C_2 \Delta x$ in Lemma A.1 and $\|\mathcal{A}_n^{-1} \mathcal{L}_{\bar{G}^n}\| \leq \sup_{t \geq 0} \frac{t}{t^2 + \lambda} = \frac{1}{2\sqrt{\lambda}}$, we have

$$\|\mathcal{A}_n^{-1} \mathcal{L}_{\bar{G}^n} (\mathcal{L}_{\bar{G}} - \mathcal{L}_{\bar{G}^n}) \phi^*\| \leq \frac{C_2 \Delta x}{2 \sqrt{\lambda}} \|\phi^*\|.$$

Since we get $\|\mathcal{L}_{\bar{G}} (\phi^* - \phi_\lambda^\infty)\| = \|\lambda \mathcal{L}_{\bar{G}} (\mathcal{L}_{\bar{G}}^2 + \lambda I)^{-1} \phi^*\| \leq \sup_{t \geq 0} \frac{\lambda t}{t^2 + \lambda} \|\phi^*\| \leq \frac{\sqrt{\lambda}}{2} \|\phi^*\|$ from (A.3),

$$\begin{aligned} \|\mathcal{A}_n^{-1} (\mathcal{L}_{\bar{G}^n}^2 - \mathcal{L}_{\bar{G}}^2) (\phi^* - \phi_\lambda^\infty)\| &\leq \|\mathcal{A}_n^{-1} \mathcal{L}_{\bar{G}^n} (\mathcal{L}_{\bar{G}^n} - \mathcal{L}_{\bar{G}}) (\phi^* - \phi_\lambda^\infty)\| + \|\mathcal{A}_n^{-1} (\mathcal{L}_{\bar{G}^n} - \mathcal{L}_{\bar{G}}) \mathcal{L}_{\bar{G}} (\phi^* - \phi_\lambda^\infty)\| \\ &\leq \frac{C_2 \Delta x}{2 \sqrt{\lambda}} \|\phi^* - \phi_\lambda^\infty\| + \frac{C_2 \Delta x}{2 \sqrt{\lambda}} \|\phi^*\|, \end{aligned}$$

based on $\mathcal{L}_{\bar{G}^n}^2 - \mathcal{L}_{\bar{G}}^2 = \mathcal{L}_{\bar{G}^n} (\mathcal{L}_{\bar{G}^n} - \mathcal{L}_{\bar{G}}) + (\mathcal{L}_{\bar{G}^n} - \mathcal{L}_{\bar{G}}) \mathcal{L}_{\bar{G}}$. By source condition in Assumption H3 and regularization error in Lemma 3.5, $\|\phi^*\| \leq C_1^{\beta/2} R$ and $\|\phi^* - \phi_\lambda^\infty\| \leq C(\beta, C_1) R \lambda^{\min\{\beta/4, 1\}}$, so

$$\|\mathcal{A}_n^{-1} (\mathcal{L}_{\bar{G}^n} - \mathcal{L}_{\bar{G}}) \phi^D + \mathcal{A}_n^{-1} (\mathcal{A} - \mathcal{A}_n) \phi_\lambda^\infty\| \leq C_2 C_1^{\beta/2} R \frac{\Delta x}{\sqrt{\lambda}} + \frac{C_2}{2} C(\beta, C_1) R \Delta x \lambda^{-1/2 + \min\{\beta/4, 1\}}.$$

For $0 < \lambda \leq 1$, $\Delta x \lambda^{-1/2 + \min\{\beta/4, 1\}} \leq \Delta x \lambda^{-1/2}$ with $\min\{\beta/4, 1\} \in [0, 1]$. Hence, the term $\Delta x \lambda^{-1/2 + \min\{\beta/4, 1\}}$ can be absorbed into $\Delta x \lambda^{-1/2}$ by adjusting the constant, yielding the final bound. Combing the bounds,

$$\left\| \hat{\phi}_\lambda^n - \phi_\lambda^\infty \right\|_{L^2_\rho} \leq C_L \Delta x \sqrt{\frac{\mathcal{N}(\lambda)}{\lambda}} + C_L \sqrt{2C_1 C_2} \frac{\Delta x^{3/2}}{\lambda} + C_\beta \frac{\Delta x}{\sqrt{\lambda}},$$

where $C_\beta = C_2 C_1^{\beta/2} R + \frac{C_2}{2} C(\beta, C_1) R$. ■

Proof of Lemma 3.7 (Numerical error). Given by the definitions of $\hat{\phi}_\lambda^n$ and $\hat{\phi}_\lambda^{n,M}$ in (3.4), add and subtract $\mathcal{A}_M^{-1}\mathcal{L}_{\bar{G}^M}\phi^{D,n}$:

$$\hat{\phi}_\lambda^{n,M} - \hat{\phi}_\lambda^n = \mathcal{A}_M^{-1}\mathcal{L}_{\bar{G}^M}(\phi^{D,M} - \phi^{D,n}) + (\mathcal{A}_M^{-1}\mathcal{L}_{\bar{G}^M} - \mathcal{A}_n^{-1}\mathcal{L}_{\bar{G}^n})\phi^{D,n},$$

where $\mathcal{A}_n := \mathcal{B}_n + \lambda I$, $\mathcal{A}_M := \mathcal{B}_M + \lambda I$ with $\mathcal{B}_n := \mathcal{L}_{\bar{G}^n}^2$, $\mathcal{B}_M := \mathcal{L}_{\bar{G}^M}^2$. For the second term, use the resolvent identity:

$$\mathcal{A}_M^{-1}\mathcal{L}_{\bar{G}^M} - \mathcal{A}_n^{-1}\mathcal{L}_{\bar{G}^n} = \mathcal{A}_M^{-1}(\mathcal{L}_{\bar{G}^M} - \mathcal{L}_{\bar{G}^n}) + \mathcal{A}_M^{-1}(\mathcal{B}_n - \mathcal{B}_M)\mathcal{A}_n^{-1}\mathcal{L}_{\bar{G}^n}.$$

Thus

$$\begin{aligned} \hat{\phi}_\lambda^{n,M} - \hat{\phi}_\lambda^n &= \underbrace{\mathcal{A}_M^{-1}\mathcal{L}_{\bar{G}^M}(\phi^{D,M} - \phi^{D,n})}_{T_1} + \underbrace{\mathcal{A}_M^{-1}(\mathcal{L}_{\bar{G}^M} - \mathcal{L}_{\bar{G}^n})\phi^{D,n}}_{T_2} \\ &\quad + \underbrace{\mathcal{A}_M^{-1}(\mathcal{B}_n - \mathcal{B}_M)\mathcal{A}_n^{-1}\mathcal{L}_{\bar{G}^n}\phi^{D,n}}_{T_3}. \end{aligned}$$

Step 1: bound for T_1 . By the effective-dimension inequality for \mathcal{A}_M and $\mathcal{L}_{\bar{G}^M}$ in Lemma A.2,

$$\|T_1\|_{L_\rho^2} = \|\mathcal{A}_M^{-1}\mathcal{L}_{\bar{G}^M}(\phi^{D,M} - \phi^{D,n})\|_{L_\rho^2} \leq \sqrt{\frac{\mathcal{N}_M(\lambda)}{\lambda}} \|\phi^{D,M} - \phi^{D,n}\|_{L_\rho^2}.$$

By definitions of $\langle \phi^{D,n}, \phi \rangle_{L_\rho^2}$ in (3.6) and $\langle \phi^{D,M}, \phi \rangle_{L_\rho^2}$ in (3.2), with $R_\phi^M[p_{t_i}](x_m) = R_\phi^n[p_{t_i}](x_m)$,

$$\begin{aligned} |\langle \phi^{D,M} - \phi^{D,n}, \phi \rangle_{L_\rho^2}| &= \left| \frac{1}{N} \sum_{i=1}^N \sum_{m=1}^M R_\phi^M[p_{t_i}](x_m) \tilde{f}_{t_i}(x_m) \Delta x - \frac{1}{N} \sum_{i=1}^N \int_{\Omega_{R_0}} R_\phi^n[p_{t_i}](x) f_{t_i}(x) dx \right| \\ &\leq A_1 + A_2, \end{aligned}$$

with

$$\begin{aligned} A_1 &:= \left| \frac{1}{N} \sum_{i=1}^N \sum_{m=1}^M R_\phi^n[p_{t_i}](x_m) (\tilde{f}_{t_i}(x_m) - f_{t_i}(x_m)) \Delta x \right|, \\ A_2 &:= \left| \frac{1}{N} \sum_{i=1}^N \sum_{m=1}^M R_\phi^n[p_{t_i}](x_m) f_{t_i}(x_m) \Delta x - \frac{1}{N} \sum_{i=1}^N \int_{\Omega_{R_0}} R_\phi^n[p_{t_i}](x) f_{t_i}(x) dx \right|. \end{aligned}$$

The key step in bounding A_1 is to control $f_{t_i}(x_m) - \tilde{f}_{t_i}(x_m)$, which decomposes into three contributions: the time derivative, the first spatial derivative and the second spatial derivative. Let $w_1(x) = b(x)p(x, t_i)$ and $w_1(x) = \sigma^2(x)p(x, t_i)$. By Taylor expansion in time and space,

$$\begin{aligned} \left| \partial_t p(t_i, x_m) - \frac{p(t_{i+1}, x_m) - p(t_i, x_m)}{\Delta t} \right| &= \frac{\Delta t}{2} |\partial_t^2 p(\tau, x_m)| \leq \frac{\Delta t}{2} \sup_{s \in [t_i, t_{i+1}]} |\partial_t^2 p(s, x_m)| \\ \left| \partial_x w_1(x_m) - \frac{w_1(x_{m+1}) - w_1(x_{m-1}))}{2\Delta x} \right| &\leq \frac{\Delta x^2}{6} \sup_{\xi \in [x_{m-1}, x_{m+1}]} |\partial_x^3 w_1(\xi)| \\ \left| \partial_x^2 w_2(x_m) - \frac{w_2(x_{m+1}) - 2w_2(x_m) + w_2(x_{m-1}))}{\Delta x^2} \right| &\leq \frac{\Delta x^2}{12} \sup_{\zeta \in [x_{m-1}, x_{m+1}]} |\partial_x^4 w_2(\zeta)| \end{aligned} \tag{A.6}$$

By the triangle inequality, we get

$$\left| f_{t_i}(x_m) - \tilde{f}_{t_i}(x_m) \right| \leq C_t \Delta t + C_w \Delta x^2, \tag{A.7}$$

where C_t and C_w depend only on bounds of $\partial_t^2 p$, $\partial_x^3(bp)$ and $\partial_x^4(\sigma^2 p)$ from Remark (3.4). Using the bound $\|R_\phi^n[p_{t_i}]\|_\infty = \sup_x |\sum_{\ell=1}^n \int Q[p_{t_i}](x, r_\ell) \mathbf{1}_{I_\ell}(r) \phi(r) dr| \leq 4C_{\max} \sqrt{\frac{R_0}{\rho_0}} \|\phi\|_{L_\rho^2}$, which follows from Cauchy-Schwarz inequality applied to $\int_\delta^{R_0} |\phi(r)| dr$, together with (A.6) and Assumption H2, we have

$$\begin{aligned} A_1 &\leq \frac{1}{N} \sum_{i=1}^N \|R_\phi^n[p_{t_i}]\|_\infty (C_t \Delta t + C_w \Delta x^2) \sum_{m=1}^M \Delta x \\ &\leq 4C_{\max} \sqrt{\frac{R_0}{\rho_0}} |\Omega_{R_0}| (C_t \Delta t + C_w \Delta x^2) \|\phi\|_{L_\rho^2}. \end{aligned}$$

For A_2 , set $b_i(x) := R_\phi^n[p_{t_i}](x) f_{t_i}(x)$. A standard quadrature error estimate yields

$$\left| \int_{\Omega_{R_0}} b_i(x) dx - \sum_{m=1}^M b_i(x_m) \Delta x \right| \leq \frac{1}{2} \|b'_i\|_\infty |\Omega_{R_0}| \Delta x.$$

Using $\|b'_i\|_\infty \leq \|\partial_x R_\phi^n[p_{t_i}]\|_\infty \|f_{t_i}\|_\infty + \|R_\phi^n[p_{t_i}]\|_\infty \|\partial_x f_{t_i}\|_\infty$ and the bounds

$$\|R_\phi^n[p_{t_i}]\|_\infty \leq 4C_{\max} \sqrt{\frac{R_0}{\rho_0}} \|\phi\|_{L_\rho^2}, \quad \|\partial_x R_\phi^n[p_{t_i}]\|_\infty \leq 4C'_{\max} \sqrt{\frac{R_0}{\rho_0}} \|\phi\|_{L_\rho^2},$$

we obtain

$$A_2 \leq 4(C'_{\max} C_0 + C_{\max} C_1) |\Omega_{R_0}| \sqrt{\frac{R_0}{\rho_0}} \|\phi\|_{L_\rho^2} \Delta x.$$

Altogether,

$$|\langle \phi^{D,M} - \phi^{D,n}, \phi \rangle_{L_\rho^2}| \leq 4 \sqrt{\frac{R_0}{\rho_0}} |\Omega_{R_0}| \left[C_{\max} (C_t \Delta t + C_w \Delta x^2) + (C'_{\max} C_0 + C_{\max} C_1) \Delta x \right] \|\phi\|_{L_\rho^2}.$$

Taking the supremum over $\|\phi\|_{L_\rho^2} = 1$ gives a bound for $\|\phi^{D,M} - \phi^{D,n}\|_{L_\rho^2}$ and thus,

$$\|T_1\|_{L_\rho^2} \leq 4 \sqrt{\frac{R_0}{\rho_0}} |\Omega_{R_0}| \left[C_{\max} (C_t \Delta t + C_w \Delta x^2) + (C'_{\max} C_0 + C_{\max} C_1) \Delta x \right] \sqrt{\frac{\mathcal{N}_M(\lambda)}{\lambda}}.$$

Step 2: bound for T_2 . Under Assumption H2, we have $\rho(r) = \rho_0$. From

$$|\langle \phi^{D,n}, \phi \rangle_{L_\rho^2}| \leq \frac{1}{N} \sum_{i=1}^N \int_{\Omega_{R_0}} |R_\phi^n[p_{t_i}](x)| |f_{t_i}(x)| dx \leq 4C_{\max} C_0 |\Omega_{R_0}| \sqrt{\frac{R_0}{\rho_0}} \|\phi\|_{L_\rho^2},$$

we get $\|\phi^{D,n}\|_{L_\rho^2} \leq 4C_{\max} C_0 |\Omega_{R_0}| \sqrt{\frac{R_0}{\rho_0}}$. Then, by Lemma A.1,

$$\begin{aligned} \|T_2\|_{L_\rho^2} &= \|\mathcal{A}_M^{-1} (\mathcal{L}_{\bar{G}^M} - \mathcal{L}_{\bar{G}^n}) \phi^{D,n}\|_{L_\rho^2} \\ &\leq \|\mathcal{A}_M^{-1}\| \|\mathcal{L}_{\bar{G}^M} - \mathcal{L}_{\bar{G}^n}\| \|\phi^{D,n}\|_{L_\rho^2} \leq 4C_{\max} C_0 C_2 |\Omega_{R_0}| \sqrt{\frac{R_0}{\rho_0}} \frac{\Delta x}{\lambda}. \end{aligned}$$

Step 3: bound for T_3 . By the source condition and $\|\mathcal{L}_{\bar{G}}\| \leq C_1$ in Lemma A.1, we have

$$\|\phi_\lambda^\infty\|_{L_\rho^2} \leq \sup_{t \in \sigma(\mathcal{B})} \frac{t^{1+\beta/4}}{t+\lambda} \|w\|_{L_\rho^2} \leq \sup_{t \in \sigma(\mathcal{B})} t^{\beta/4} \|w\|_{L_\rho^2} \leq C_1^{\beta/2} R.$$

Using the bound on $\|\hat{\phi}_\lambda^n - \phi_\lambda^\infty\|_{L_\rho^2}$ in Lemma 3.6 and the bound on $\|\phi_\lambda^\infty\|_{L_\rho^2}$,

$$\begin{aligned} \|\mathcal{A}_n^{-1} \mathcal{L}_{\bar{G}^n} \phi^{D,n}\|_{L_\rho^2} &= \|\hat{\phi}_\lambda^n\|_{L_\rho^2} \leq \|\hat{\phi}_\lambda^n - \phi_\lambda^\infty\|_{L_\rho^2} + \|\phi_\lambda^\infty\|_{L_\rho^2} \\ &\leq C_L \Delta x \sqrt{\frac{\mathcal{N}(\lambda)}{\lambda}} + C_L \sqrt{2C_1 C_2} \frac{\Delta x^{3/2}}{\lambda} + C_\beta \frac{\Delta x}{\sqrt{\lambda}} + C_1^{\beta/2} R. \end{aligned}$$

Combining the bound of $\|\mathcal{B}_n - \mathcal{B}_M\|$ from Lemma A.1 and the bound of $\|\mathcal{A}_n^{-1} \mathcal{L}_{\bar{G}^n} \phi^{D,n}\|_{L_\rho^2}$,

$$\begin{aligned} \|T_3\|_{L_\rho^2} &= \|\mathcal{A}_M^{-1} (\mathcal{B}_n - \mathcal{B}_M) \mathcal{A}_n^{-1} \mathcal{L}_{\bar{G}^n} \phi^{D,n}\|_{L_\rho^2} \\ &\leq \|\mathcal{A}_M^{-1}\| \|\mathcal{B}_n - \mathcal{B}_M\| \|\mathcal{A}_n^{-1} \mathcal{L}_{\bar{G}^n} \phi^{D,n}\|_{L_\rho^2} \\ &\leq \frac{\Delta x C_1 C_2}{\lambda} \left(C_L \Delta x \sqrt{\frac{\mathcal{N}(\lambda)}{\lambda}} + C_L \sqrt{2C_1 C_2} \frac{\Delta x^{3/2}}{\lambda} + C_\beta \frac{\Delta x}{\sqrt{\lambda}} + C_1^{\beta/2} R \right) \end{aligned}$$

Step 4: collect the bounds. From Lemma A.3 and (A.5) we know that $\sqrt{\frac{\mathcal{N}_M(\lambda)}{\lambda}} \leq \sqrt{\frac{\mathcal{N}_n(\lambda)}{\lambda}} + \sqrt{\frac{2C_1 C_2}{\lambda^2}} \Delta x \leq \sqrt{\frac{\mathcal{N}(\lambda)}{\lambda}} + 2\sqrt{\frac{2C_1 C_2}{\lambda^2}} \Delta x$. Putting together the bounds for T_1 , T_2 , and T_3 and substituting the above estimates for $\sqrt{\mathcal{N}_M(\lambda)/\lambda}$ and $\sqrt{\mathcal{N}_n(\lambda)/\lambda}$, we obtain

$$\begin{aligned} \|\hat{\phi}_\lambda^{n,M} - \hat{\phi}_\lambda^n\|_{L_\rho^2} &\leq \|T_1\|_{L_\rho^2} + \|T_2\|_{L_\rho^2} + \|T_3\|_{L_\rho^2} \\ &\leq K_1 (\Delta t + \Delta x + \Delta x^2) \left(\sqrt{\frac{\mathcal{N}(\lambda)}{\lambda}} + \sqrt{\frac{\Delta x}{\lambda^2}} \right) \\ &\quad + K_2 \frac{\Delta x}{\lambda} + K_3 \frac{\Delta x^2}{\lambda} \sqrt{\frac{\mathcal{N}(\lambda)}{\lambda}} + K_4 \frac{\Delta x^{5/2}}{\lambda^2} + K_5 \frac{\Delta x^2}{\lambda^{3/2}} \end{aligned}$$

where the constants $K_i > 0$ are independent of Δx , Δt and λ . This completes the proof. ■

A.3 Technical lemmas and their proofs

Lemma A.1 Under Assumptions H1' and H2, the kernels $\bar{G}, \bar{G}^n, \bar{G}^M$, defined in (2.10), (3.5), (2.21), are in $L^2(\rho \otimes \rho)$ with norms bounded by C_1 , so their integral operators $\mathcal{L}_{\bar{G}}, \mathcal{L}_{\bar{G}^n}, \mathcal{L}_{\bar{G}^M}$ have norms bounded by C_1 . Moreover,

$$\|\mathcal{L}_{\bar{G}} - \mathcal{L}_{\bar{G}^n}\| \leq \|\bar{G} - \bar{G}^n\|_{L^2(\rho \otimes \rho)} \leq C_2 \Delta x, \quad (\text{A.8})$$

$$\|\mathcal{L}_{\bar{G}^n} - \mathcal{L}_{\bar{G}^M}\| \leq \|\bar{G}^n - \bar{G}^M\|_{L^2(\rho \otimes \rho)} \leq C_2 \Delta x, \quad (\text{A.9})$$

with $C_1 = 4C_{\max} Z$, $C_2 = \frac{16C_{\max} |\Omega_{R_0}| C'_{\max}}{\rho_0^2}$ and $\Delta x = \Delta r$.

Proof of Lemma A.1. Based on the definition of \bar{G} in (2.10) and Assumption H1,

$$\|\bar{G}\|_{L^2(\rho \otimes \rho)}^2 = \iint |\bar{G}(r, s)|^2 \rho(r)\rho(s) dr ds \leq 16C_{\max}^2 Z^2$$

so $\|\bar{G}\|_{L^2(\rho \otimes \rho)} \leq C_1$. Similarly, $\|\bar{G}^n\|_{L^2(\rho \otimes \rho)}, \|\bar{G}^M\|_{L^2(\rho \otimes \rho)} \leq C_1$. Then, by the definition of $\mathcal{L}_{\bar{G}}$ in (2.11), for any $\phi \in L_\rho^2$

$$|(\mathcal{L}_{\bar{G}}\phi)(r)| = \left| \int \bar{G}(r, s)\phi(s)\rho(s) ds \right| \leq \left(\int |\bar{G}(r, s)|^2 \rho(s) ds \right)^{1/2} \|\phi\|_{L_\rho^2}$$

by Cauchy-Schwarz. Squaring and integrating in r against $\rho(r)dr$ gives

$$\|\mathcal{L}_{\bar{G}}\phi\|_{L_\rho^2}^2 \leq \left(\iint |\bar{G}(r, s)|^2 \rho(r)\rho(s) dr ds \right) \|\phi\|_{L_\rho^2}^2 = \|\bar{G}\|_{L^2(\rho \otimes \rho)}^2 \|\phi\|_{L_\rho^2}^2$$

Taking $\sup_{\phi \neq 0}$ yields $\|\mathcal{L}_{\bar{G}}\| \leq \|\bar{G}\|_{L^2(\rho \otimes \rho)}$. Applying the same argument to \bar{G}^n proves $\|\mathcal{L}_{\bar{G}^n}\| \leq \|\bar{G}^n\|_{L^2(\rho \otimes \rho)}$. The same argument with \bar{G} replaced by $\bar{G} - \bar{G}^n$ gives $\|\mathcal{L}_{\bar{G}} - \mathcal{L}_{\bar{G}^n}\| \leq \|\bar{G} - \bar{G}^n\|_{L^2(\rho \otimes \rho)}$. Finally, by Remark 3.4, for any x ,

$$|Q[p_{t_i}](x, s_k) - Q[p_{t_i}](x, s)| \leq |p_{t_i}(x + s_k) - p_{t_i}(x + s)| + |p_{t_i}(x - s_k) - p_{t_i}(x - s)| \leq 2C'_{\max} \Delta r.$$

Thus, for $(r, s) \in I_{k'} \times I_k$,

$$\begin{aligned} |G(r_{k'}, s_k) - G(r, s)| &\leq \frac{1}{N} \sum_{i=1} \int_{\Omega_{R_0}} |Q[p_{t_i}](x, r_{k'})| |Q[p_{t_i}](x, s_k) - Q[p_{t_i}](x, s)| dx \\ &\quad + \frac{1}{N} \sum_{i=1} \int_{\Omega_{R_0}} |Q[p_{t_i}](x, s)| |Q[p_{t_i}](x, r_{k'}) - Q[p_{t_i}](x, r)| dx \\ &\leq 16C_{\max} |\Omega_{R_0}| C'_{\max} \Delta r, \end{aligned}$$

with $|Q[p_{t_i}](x, r)| \leq 4C_{\max}, \forall x, r$. Under Assumption H2, $\rho(r) = \rho_0$. Using the definition of \bar{G}^n in (3.5),

$$\begin{aligned} \|\bar{G}^n - \bar{G}\|_{L^2(\rho \otimes \rho)}^2 &= \sum_{k', k} \iint_{I_{k'} \times I_k} \frac{|G(r_{k'}, s_k) - G(r, s)|^2}{\rho(r)\rho(s)} dr ds \\ &\leq \left(\frac{16C_{\max} |\Omega_{R_0}| C'_{\max} \Delta r}{\rho_0^2} \right)^2 \sum_{k', k} \iint_{I_{k'} \times I_k} \rho(r)\rho(s) dr ds \\ &= \left(\frac{16C_{\max} |\Omega_{R_0}| C'_{\max}}{\rho_0^2} \right)^2 (\Delta r)^2 \end{aligned}$$

with $\sum_{k', k} \iint_{I_{k'} \times I_k} \rho(r)\rho(s) dr ds = \iint \rho(r)\rho(s) dr ds = 1$. Taking square roots gives $\|\bar{G}^n - \bar{G}\|_{L^2(\rho \otimes \rho)} \leq C_2 \Delta r$.

The bound for $\|\mathcal{L}_{\bar{G}^n} - \mathcal{L}_{\bar{G}^M}\|$ follows by the same argument, using the definition of \bar{G}^M in (2.21) and noting that the same estimate for $|G(r_{k'}, s_k) - G(r, s)|$ holds. ■

Lemma A.2 Let $\mathcal{L} : L_\rho^2 \rightarrow L_\rho^2$ be self-adjoint, nonnegative and Hilbert–Schmidt and set $\mathcal{A} := \mathcal{B} + \lambda I$ with $\mathcal{B} := \mathcal{L}^2$ and $\lambda > 0$. Denote the effective dimension by $\mathcal{N}(\lambda) := \text{Tr}(\mathcal{B}(\mathcal{B} + \lambda I)^{-1})$. Then, for every $\phi \in L_\rho^2$,

$$\|\mathcal{A}^{-1}\mathcal{L}\phi\|_{L_\rho^2} \leq \sqrt{\frac{\mathcal{N}(\lambda)}{\lambda}} \|\phi\|_{L_\rho^2}.$$

In particular, the same estimate holds for $\mathcal{L} = \mathcal{L}_{\overline{G}}$, for each piecewise-constant operator $\mathcal{L}_{\overline{G}^n}$ in r , and for the fully discrete operator $\mathcal{L}_{\overline{G}^M}$ in (x, r) , with effective dimensions $\mathcal{N}(\lambda)$, $\mathcal{N}_n(\lambda)$ and $\mathcal{N}_M(\lambda)$ defined in the same way from $\mathcal{L}_{\overline{G}}$, $\mathcal{L}_{\overline{G}^n}$ and $\mathcal{L}_{\overline{G}^M}$, respectively.

Proof of Lemma A.2. If $\mathcal{L} \equiv 0$, then $\mathcal{B} = 0$, $\mathcal{A} = \lambda I$ and $\mathcal{N}(\lambda) = 0$, so both sides of the inequality are zero and the claim is trivial. Hence we assume $\mathcal{L} \neq 0$.

Since \mathcal{L} is compact, self-adjoint and nonnegative, the spectral theorem yields an orthonormal basis $\{e_j\}_{j \geq 1} \subset L_\rho^2$ and eigenvalues $\sigma_j \geq 0$ such that $\mathcal{L}e_j = \sigma_j e_j$, $j = 1, 2, \dots$. Then $\mathcal{B} = \mathcal{L}^2 \Rightarrow \mathcal{B}e_j = \sigma_j^2 e_j =: \mu_j e_j$, so $\{e_j\}$ is also an eigenbasis of \mathcal{B} with eigenvalues $\mu_j = \sigma_j^2$, and

$$\mathcal{A} = \mathcal{B} + \lambda I \Rightarrow \mathcal{A}e_j = (\mu_j + \lambda)e_j, \quad \lambda > 0.$$

The Hilbert–Schmidt norm of $\mathcal{A}^{-1}\mathcal{L}$ is

$$\|\mathcal{A}^{-1}\mathcal{L}\|_{\text{HS}}^2 = \sum_{j \geq 1} \|\mathcal{A}^{-1}\mathcal{L}e_j\|_{L_\rho^2}^2 = \sum_{j \geq 1} \frac{\mu_j}{(\mu_j + \lambda)^2}.$$

For each j we have

$$\frac{\mu_j}{(\mu_j + \lambda)^2} = \frac{1}{\mu_j + \lambda} \cdot \frac{\mu_j}{\mu_j + \lambda} \leq \frac{1}{\lambda} \cdot \frac{\mu_j}{\mu_j + \lambda},$$

since $\mu_j + \lambda \geq \lambda$. Summing over j gives

$$\|\mathcal{A}^{-1}\mathcal{L}\|_{\text{HS}}^2 \leq \frac{1}{\lambda} \sum_{j \geq 1} \frac{\mu_j}{\mu_j + \lambda} = \frac{\mathcal{N}(\lambda)}{\lambda}.$$

Thus, $\|\mathcal{A}^{-1}\mathcal{L}\| \leq \|\mathcal{A}^{-1}\mathcal{L}\|_{\text{HS}} \leq \sqrt{\frac{\mathcal{N}(\lambda)}{\lambda}}$ and $\|\mathcal{A}^{-1}\mathcal{L}\phi\|_{L_\rho^2} \leq \sqrt{\frac{\mathcal{N}(\lambda)}{\lambda}} \|\phi\|_{L_\rho^2}$ for any $\phi \in L_\rho^2$.

The cases $\mathcal{L} = \mathcal{L}_{\overline{G}}$, $\mathcal{L} = \mathcal{L}_{\overline{G}^n}$ and $\mathcal{L} = \mathcal{L}_{\overline{G}^M}$ follow by applying the same argument to each operator, which only changes the eigenvalues and hence replaces $\mathcal{N}(\lambda)$ by $\mathcal{N}(\lambda)$, $\mathcal{N}_n(\lambda)$ and $\mathcal{N}_M(\lambda)$ respectively. ■

Lemma A.3 Let $\mathcal{B} := \mathcal{L}_{\overline{G}}^2$ and $\mathcal{B}_n := \mathcal{L}_{\overline{G}^n}^2$, and assume $\mathcal{L}_{\overline{G}} \neq 0$. Define the effective dimensions: $\mathcal{N}(\lambda) := \text{Tr}(\mathcal{B}(\mathcal{B} + \lambda I)^{-1})$, $\mathcal{N}_n(\lambda) := \text{Tr}(\mathcal{B}_n(\mathcal{B}_n + \lambda I)^{-1})$. Then, for any fixed $\lambda > 0$,

$$|\mathcal{N}_n(\lambda) - \mathcal{N}(\lambda)| \leq \frac{2C_1 C_2}{\lambda} \Delta r.$$

Moreover, if $\mathcal{B}_M := \mathcal{L}_{\overline{G}^M}^2$ and $\mathcal{N}_M(\lambda) := \text{Tr}(\mathcal{B}_M(\mathcal{B}_M + \lambda I)^{-1})$, then the same bound applies to $|\mathcal{N}_M(\lambda) - \mathcal{N}_n(\lambda)|$.

Proof of Lemma A.3. Fix $\lambda > 0$ and define $f_\lambda(t) := t/(t + \lambda)$ for $t \geq 0$. Since \mathcal{B} and \mathcal{B}_n are self-adjoint, trace-class operators, let $\{\mu_j\}_{j \geq 1}$ and $\{\mu_{j,n}\}_{j \geq 1}$ denote their nonnegative eigenvalues, listed in non-increasing order. Then

$$|\mathcal{N}_n(\lambda) - \mathcal{N}(\lambda)| = \left| \sum_{j \geq 1} f_\lambda(\mu_{j,n}) - \sum_{j \geq 1} f_\lambda(\mu_j) \right| \leq \sum_{j \geq 1} |f_\lambda(\mu_{j,n}) - f_\lambda(\mu_j)| \leq \frac{1}{\lambda} \sum_{j \geq 1} |\mu_{j,n} - \mu_j|, \quad (\text{A.10})$$

since $|f_\lambda(a) - f_\lambda(b)| = \left| \frac{a}{a+\lambda} - \frac{b}{b+\lambda} \right| = \lambda \frac{|a-b|}{(a+\lambda)(b+\lambda)} \leq \frac{1}{\lambda} |a-b|$, for all $a, b \geq 0$. Next, by the Schatten Hölder inequality $\|AB\|_1 \leq \|A\|_2 \|B\|_2$ for Hilbert–Schmidt operators A, B , we obtain

$$\begin{aligned} \|\mathcal{B}_n - \mathcal{B}\|_1 &\leq \|\mathcal{L}_{\overline{G}^n}(\mathcal{L}_{\overline{G}^n} - \mathcal{L}_{\overline{G}})\|_1 + \|(\mathcal{L}_{\overline{G}^n} - \mathcal{L}_{\overline{G}})\mathcal{L}_{\overline{G}}\|_1 \\ &\leq \|\mathcal{L}_{\overline{G}^n}\|_2 \|\mathcal{L}_{\overline{G}^n} - \mathcal{L}_{\overline{G}}\|_2 + \|\mathcal{L}_{\overline{G}^n} - \mathcal{L}_{\overline{G}}\|_2 \|\mathcal{L}_{\overline{G}}\|_2 \leq 2C_1 C_2 \Delta r \end{aligned}$$

by using $\|\mathcal{L}_{\overline{G}^n}\|_2, \|\mathcal{L}_{\overline{G}}\|_2 \leq C_1$ and $\|\mathcal{L}_{\overline{G}^n} - \mathcal{L}_{\overline{G}}\|_2 \leq C_2 \Delta r$ in Lemma A.1. By the Mirsky inequality [44],

$$\sum_{j \geq 1} |\mu_{j,n} - \mu_j| \leq \|\mathcal{B}_n - \mathcal{B}\|_1 \leq 2C_1 C_2 \Delta r. \quad (\text{A.11})$$

Combining (A.10) and (A.11) yields

$$|\mathcal{N}_n(\lambda) - \mathcal{N}(\lambda)| \leq \frac{2C_1 C_2}{\lambda} \Delta r.$$

Similarly, applying the same argument with $(\mathcal{B}, \mathcal{B}_n)$ replaced by $(\mathcal{B}_M, \mathcal{B}_M)$ gives

$$|\mathcal{N}_M(\lambda) - \mathcal{N}_n(\lambda)| \leq \frac{2C_1 C_2}{\lambda} \Delta r.$$

■

The next lemma shows that when the eigenvalues decay polynomially with a rate $\lambda_k \sim k^{-\varsigma}$ for $\varsigma > 1/2$, the effective dimension $\mathcal{N}_{2\varsigma}(\lambda)$ increases at the order $O(\lambda^{-1/2\varsigma})$ as $\lambda \downarrow 0$.

Lemma A.4 *Assume that there exist constants $a \geq 0, b > 0$ and $\varsigma > 1/4$ such that $a k^{-2\varsigma} \leq \lambda_k \leq b k^{-2\varsigma}$, $k \in \mathbb{N}$. Then, for all $0 < \lambda < 1$, we have*

$$C_1 \lambda^{-1/(4\varsigma)} - \frac{1}{2} \leq \mathcal{N}_{4\varsigma}(\lambda) := \sum_{k \geq 1} \frac{\lambda_k^2}{\lambda_k^2 + \lambda} \leq C_2 \lambda^{-1/(4\varsigma)} + 1.$$

where $C_1 = \frac{a^{1/(2\varsigma)}}{2}$ and $C_2 = b^{1/(2\varsigma)} \left(1 + \frac{1}{4\varsigma-1}\right)$. In particular, we have $\mathcal{N}_{4\varsigma}(\lambda) \asymp \lambda^{-1/(4\varsigma)}$ as $\lambda \downarrow 0$.

Proof. Let $m(\lambda)$ be the number of $\lambda_k^2 > \lambda$, i.e.,

$$m(\lambda) := \#\{k \geq 1 : \lambda_k^2 \geq \lambda\} = \#\{k \geq 1 : \lambda_k \geq \sqrt{\lambda}\}.$$

The two-sided decay condition implies that

$$(a/\sqrt{\lambda})^{1/(2\varsigma)} - 1 \leq m(\lambda) \leq (b/\sqrt{\lambda})^{1/(2\varsigma)} + 1 =: K_b(\lambda). \quad (1)$$

Since $\frac{1}{2} \mathbf{1}_{\{x \geq 1\}} \leq \frac{x}{x+1} \leq \mathbf{1}_{\{x \geq 1\}} + x \mathbf{1}_{\{x < 1\}}$ for all $x \geq 0$, with $x = \lambda_k^2/\lambda$, we have

$$\frac{1}{2} m(\lambda) \leq \mathcal{N}_{4\varsigma}(\lambda) = \sum_{k \geq 1} \frac{\lambda_k^2/\lambda}{\lambda_k^2/\lambda + 1} \leq m(\lambda) + \frac{1}{\lambda} \sum_{k: \lambda_k^2 < \lambda} \lambda_k^2.$$

The lower bound with $C_1 = \frac{a^{1/(2\varsigma)}}{2}$ then follows directly from

$$\mathcal{N}_{4\varsigma}(\lambda) \geq \frac{1}{2} m(\lambda) \geq \frac{1}{2} \left((a/\sqrt{\lambda})^{1/(2\varsigma)} - 1 \right) = \frac{a^{1/(2\varsigma)}}{2} \lambda^{-1/(4\varsigma)} - \frac{1}{2}.$$

To control the upper bound, note that $\{k : \lambda_k^2 < \lambda\} \subset \{k > K_b(\lambda)\}$. Hence, using $\lambda_k \leq bk^{-2\varsigma}$,

$$\sum_{k: \lambda_k^2 < \lambda} \lambda_k^2 \leq \sum_{k > K_b(\lambda)} \lambda_k^2 \leq b^2 \sum_{k > K_b(\lambda)} k^{-4\varsigma}.$$

By the integral test (valid since $4\varsigma > 1$), $\sum_{k > K} k^{-4\varsigma} \leq \int_K^\infty x^{-4\varsigma} dx = \frac{K^{1-4\varsigma}}{4\varsigma-1}$. Therefore,

$$\mathcal{N}_{4\varsigma}(\lambda) \leq K_b(\lambda) + \frac{b^2}{(4\varsigma-1)\lambda} K_b(\lambda)^{1-4\varsigma} \leq b^{1/(2\varsigma)} \left(1 + \frac{1}{4\varsigma-1}\right) \lambda^{-1/(4\varsigma)} + 1,$$

which gives the upper bound with $C_2 = b^{1/(2\varsigma)} \left(1 + \frac{1}{4\varsigma-1}\right)$. ■

References

- [1] Cindy L Yu, Haitao Li, and Martin T Wells. Mcmc estimation of lévy jump models using stock and option prices. *Mathematical Finance: An International Journal of Mathematics, Statistics and Financial Economics*, 21(3):383–422, 2011.
- [2] S Kindermann, P Mayer, Hansjörg Albrecher, and H Engl. Identification of the local speed function in a lévy model for option pricing. *The Journal of Integral Equations and Applications*, pages 161–200, 2008.
- [3] D Applebaum. Lévy processes and stochastic calculus. *Cambridge Studies in Advanced Mathematics*, 116, 2009.
- [4] Yayun Zheng, Fang Yang, Jinqiao Duan, Xu Sun, Ling Fu, and Jürgen Kurths. The maximum likelihood climate change for global warming under the influence of greenhouse effect and lévy noise. *Chaos: An Interdisciplinary Journal of Nonlinear Science*, 30(1), 2020.
- [5] Yang Li, Yubin Lu, Shengyuan Xu, and Jinqiao Duan. Extracting stochastic dynamical systems with α -stable lévy noise from data. *Journal of Statistical Mechanics: Theory and Experiment*, 2022(2):023405, 2022.
- [6] Fabienne Comte and Valentine Genon-Catalot. Nonparametric estimation for pure jump lévy processes based on high frequency data. *Stochastic Processes and their Applications*, 119(12):4088–4123, 2009.
- [7] Michael H Neumann and Markus Reiß. Nonparametric estimation for lévy processes from low-frequency observations. *Bernoulli*, 15(1):223–248, 2009.
- [8] Céline Duval and Ester Mariucci. Spectral-free estimation of lévy densities in high-frequency regime. *Bernoulli*, 27(4):2649–2674, 2021.
- [9] Céline Duval, Taher Jalal, and Ester Mariucci. Adaptive minimax estimation for discretely observed lévy processes. *arXiv preprint arXiv:2411.00253*, 2024.
- [10] Céline Duval, Jalal Taher, and Ester Mariucci. Nonparametric density estimation for the small jumps of lévy processes. *Statistical Inference for Stochastic Processes*, 28(3):1–26, 2025.
- [11] Yang Li and Jinqiao Duan. A data-driven approach for discovering stochastic dynamical systems with non-gaussian lévy noise. *Physica D: Nonlinear Phenomena*, 417:132830, 2021.
- [12] Yubin Lu, Yang Li, and Jinqiao Duan. Extracting stochastic governing laws by non-local kramers-moyal formulae. *Philosophical Transactions of the Royal Society A*, 380(2229):20210195, 2022.
- [13] Guofei Pang, Marta D’Elia, Michael Parks, and George E Karniadakis. npinns: nonlocal physics-informed neural networks for a parametrized nonlocal universal laplacian operator. algorithms and applications. *Journal of Computational Physics*, 422:109760, 2020.

- [14] Huaiqian You, Yue Yu, Marta D’Elia, Tian Gao, and Stewart Silling. Nonlocal kernel network (nkn): A stable and resolution-independent deep neural network. *Journal of Computational Physics*, 469:111536, 2022.
- [15] Huaiqian You, Yue Yu, Nathaniel Trask, Mamikon Gulian, and Marta D’Elia. Data-driven learning of nonlocal physics from high-fidelity synthetic data. *Computer Methods in Applied Mechanics and Engineering*, 374:113553, 2021.
- [16] Yiming Fan, Marta D’Elia, Yue Yu, Habib N Najm, and Stewart Silling. Bayesian nonlocal operator regression: A data-driven learning framework of nonlocal models with uncertainty quantification. *Journal of Engineering Mechanics*, 149(8):04023049, 2023.
- [17] Fei Lu, Quanjun Lang, and Qingci An. Data adaptive rkhs tikhonov regularization for learning kernels in operators. In *Mathematical and Scientific Machine Learning*, pages 158–172. PMLR, 2022.
- [18] Chao Zhang and Dacheng Tao. Risk bounds of learning processes for lévy processes. *Journal of Machine Learning Research*, 2013.
- [19] Heinz Werner Engl, Martin Hanke, and Andreas Neubauer. *Regularization of Inverse Problems*. Mathematics and Its Applications. Springer Dordrecht, 1996.
- [20] Gilles Blanchard and Nicole Mücke. Optimal rates for regularization of statistical inverse learning problems. *Foundations of Computational Mathematics*, 18(4):971–1013, 2018.
- [21] Sichong Zhang, Xiong Wang, and Fei Lu. Minimax rate for learning kernels in operators. *arXiv preprint arXiv:2502.20368*, 2025.
- [22] Nicholas H Nelsen, Houman Owhadi, Andrew M Stuart, Xianjin Yang, and Zongren Zou. Bilevel optimization for learning hyperparameters: Application to solving pdes and inverse problems with gaussian processes. *arXiv preprint arXiv:2510.05568*, 2025.
- [23] Neil K Chada, Claudia Schillings, Xin T Tong, and Simon Weissmann. Consistency analysis of bilevel data-driven learning in inverse problems. *Communications in Mathematical Sciences*, 20(1):123–164, 2022.
- [24] Per Christian Hansen. Analysis of discrete ill-posed problems by means of the l-curve. *SIAM review*, 34(4):561–580, 1992.
- [25] Gene H Golub, Michael Heath, and Grace Wahba. Generalized cross-validation as a method for choosing a good ridge parameter. *Technometrics*, 21(2):215–223, 1979.
- [26] Fei Lu, Qingci An, and Yue Yu. Nonparametric learning of kernels in nonlocal operators. *Journal of Peridynamics and Nonlocal Modeling*, pages 1–24, 2023.
- [27] Quanjun Lang and Fei Lu. Learning interaction kernels in mean-field equations of first-order systems of interacting particles. *SIAM Journal on Scientific Computing*, 44(1):A260–A285, 2022.
- [28] Zhen-Qing Chen, Eryan Hu, Longjie Xie, and Xicheng Zhang. Heat kernels for non-symmetric diffusion operators with jumps. *Journal of Differential Equations*, 263(10):6576–6634, 2017.
- [29] Felipe Cucker and Ding Xuan Zhou. *Learning theory: an approximation theory viewpoint*, volume 24. Cambridge University Press, 2007.
- [30] Haibo Li and Fei Lu. Automatic reproducing kernel and regularization for learning convolution kernels. *arXiv preprint arXiv:2507.11944*, 2025.
- [31] Darko Volkov. Optimal decay rates in sobolev norms for singular values of integral operators. *Journal of Mathematical Analysis and Applications*, 537(2):128403, 2024.
- [32] Andrea Caponnetto and Ernesto De Vito. Optimal rates for the regularized least-squares algorithm. *Foundations of Computational Mathematics*, 7(3):331–368, 2007.

- [33] Tong Zhang. Learning bounds for kernel regression using effective data dimensionality. *Neural computation*, 17(9):2077–2098, 2005.
- [34] Gernot Holler, Karl Kunisch, and Richard C Barnard. A bilevel approach for parameter learning in inverse problems. *Inverse Problems*, 34(11):115012, 2018.
- [35] Diederik P Kingma and Jimmy Ba. Adam: A method for stochastic optimization. *arXiv preprint arXiv:1412.6980*, 2014.
- [36] Risheng Liu, Jiaxin Gao, Jin Zhang, Deyu Meng, and Zhouchen Lin. Investigating bi-level optimization for learning and vision from a unified perspective: A survey and beyond. *IEEE Transactions on Pattern Analysis and Machine Intelligence*, 44(12):10045–10067, 2021.
- [37] Jonathan Lorraine, Paul Vicol, and David Duvenaud. Optimizing millions of hyperparameters by implicit differentiation. In *International conference on artificial intelligence and statistics*, pages 1540–1552. PMLR, 2020.
- [38] Aravind Rajeswaran, Chelsea Finn, Sham M Kakade, and Sergey Levine. Meta-learning with implicit gradients. *Advances in neural information processing systems*, 32, 2019.
- [39] Per Christian Hansen. Regularization tools: A matlab package for analysis and solution of discrete ill-posed problems. *Numerical algorithms*, 6(1):1–35, 1994.
- [40] Yurii Nesterov. A method for solving the convex programming problem with convergence rate $o(1/k^2)$. In *Dokl akad nauk Sssr*, volume 269, page 543, 1983.
- [41] Atilim Gunes Baydin, Robert Cornish, David Martinez Rubio, Mark Schmidt, and Frank Wood. Online learning rate adaptation with hypergradient descent. In *International Conference on Learning Representations*, 2018.
- [42] Philip Protter and Denis Talay. The euler scheme for lévy driven stochastic differential equations. *The Annals of Probability*, 25(1):393–423, 1997.
- [43] Abraham Savitzky and Marcel JE Golay. Smoothing and differentiation of data by simplified least squares procedures. *Analytical chemistry*, 36(8):1627–1639, 1964.
- [44] Simon Foucart. Concave mirsky inequality and low-rank recovery. *SIAM Journal on Matrix Analysis and Applications*, 39(1):99–103, 2018.